



Radio interferometry - Brief history, theory & practice

Sándor Frey

`frey@sgo.fomi.hu`

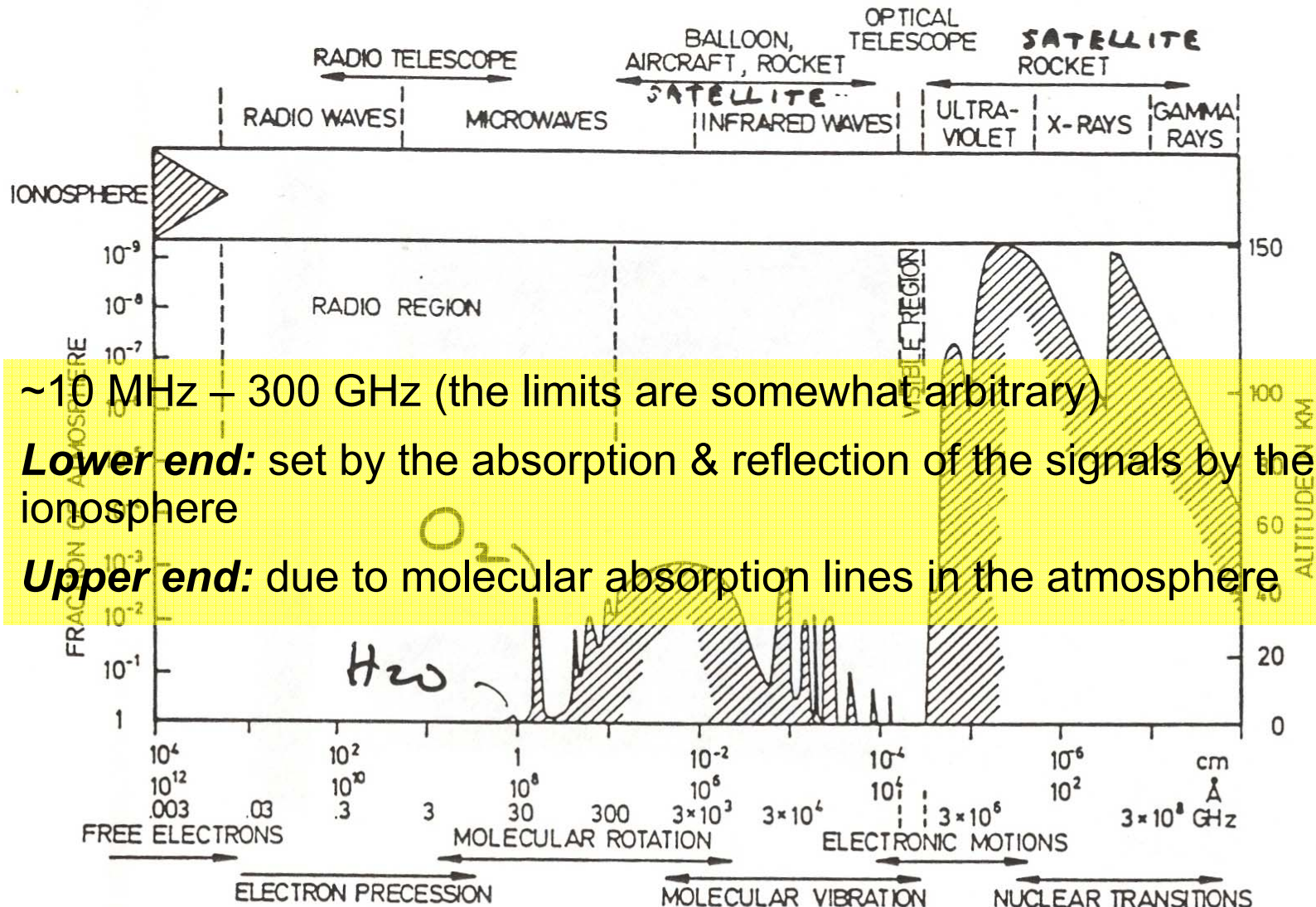
**Institute of Geodesy, Cartography
and Remote Sensing (FÖMI)
Satellite Geodetic Observatory**

***Astrometry and Imaging with the VLTI – Summer School
Keszthely, 5 June 2008***

The outline of the talk

- Radio astronomy & radio telescopes
- Why interferometry?
- Brief history of radio interferometers
- Optical vs. radio interferometry – differences
- Science with radio interferometry
- Interferometer arrays – available & planned
- Image reconstruction basics: methods, software
- **Practical demo session (*later, if you survive...*)**

The atmospheric radio window

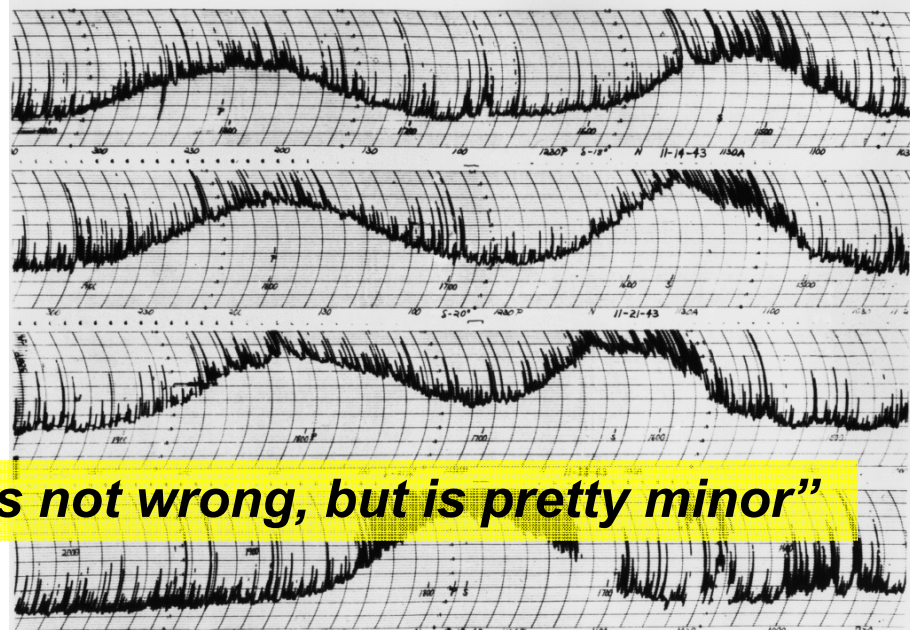
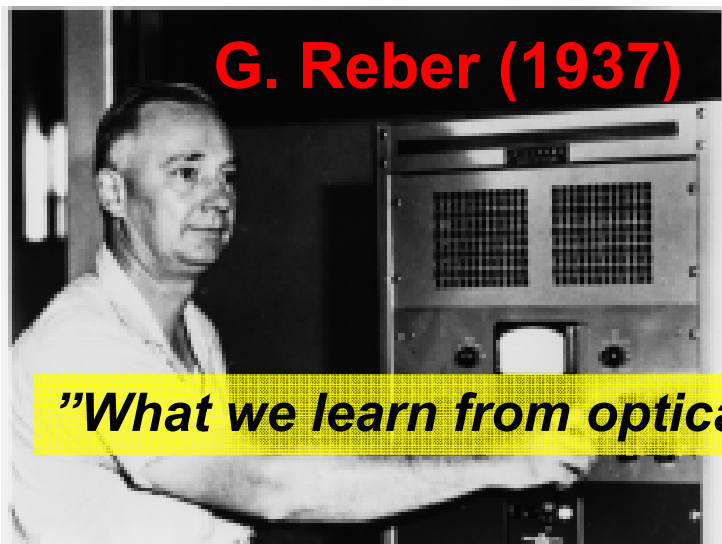
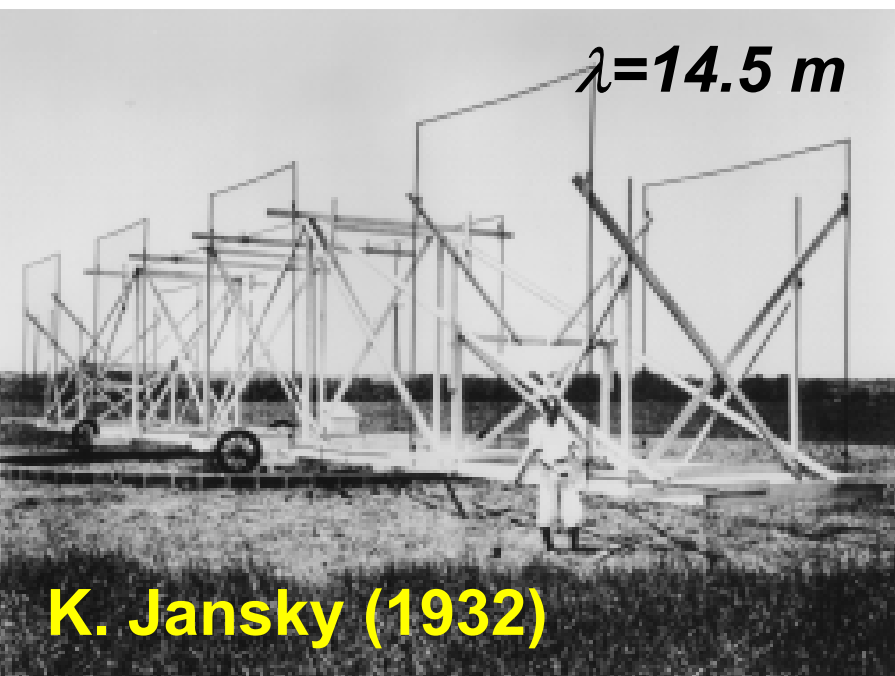


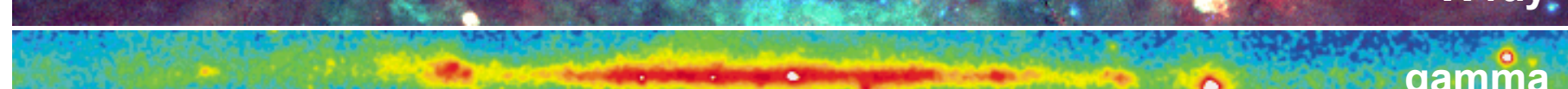
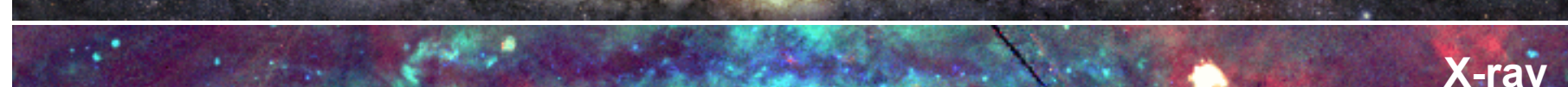
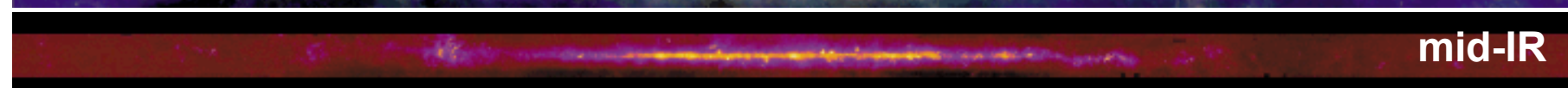
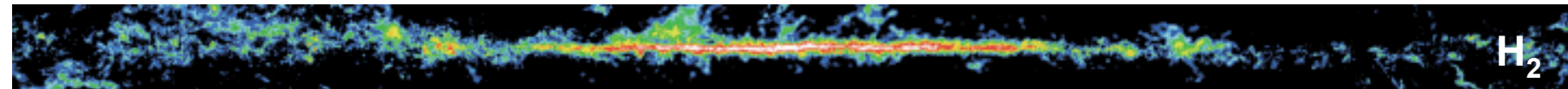
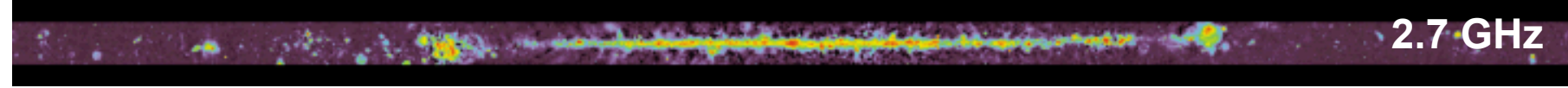
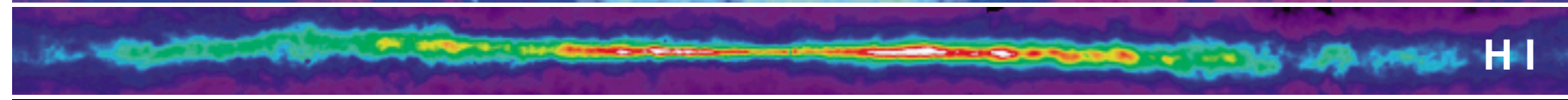
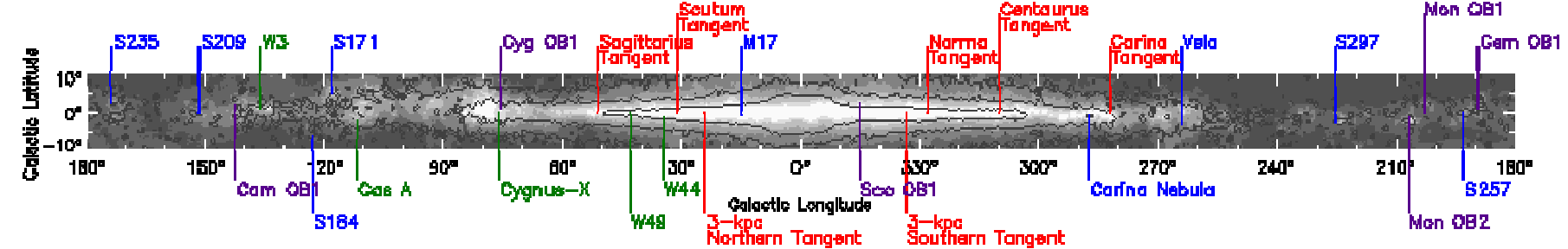
~10 MHz – 300 GHz (the limits are somewhat arbitrary)

Lower end: set by the absorption & reflection of the signals by the ionosphere

Upper end: due to molecular absorption lines in the atmosphere

Fig. 1.1. The transmission of the earth atmosphere for electromagnetic radiation. The diagram gives the height in the atmosphere at which the radiation is attenuated by a factor 1/2





Radio telescopes

- Dipole arrays
- Reflectors (mostly paraboloid dishes)

Typical properties of reflectors:

can be directed towards any point on the sky

steerable dishes to track sources' apparent motion

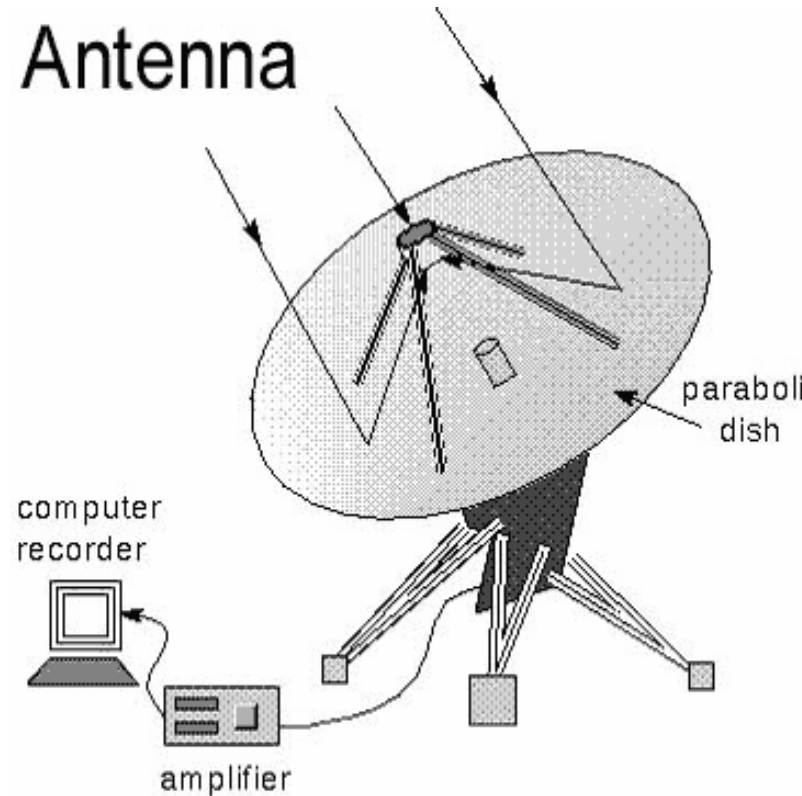
radiation is reflected (metal surface) and focused

surface accuracy needed depends on the wavelength

dipole at the focus (primary or Cassegrain)

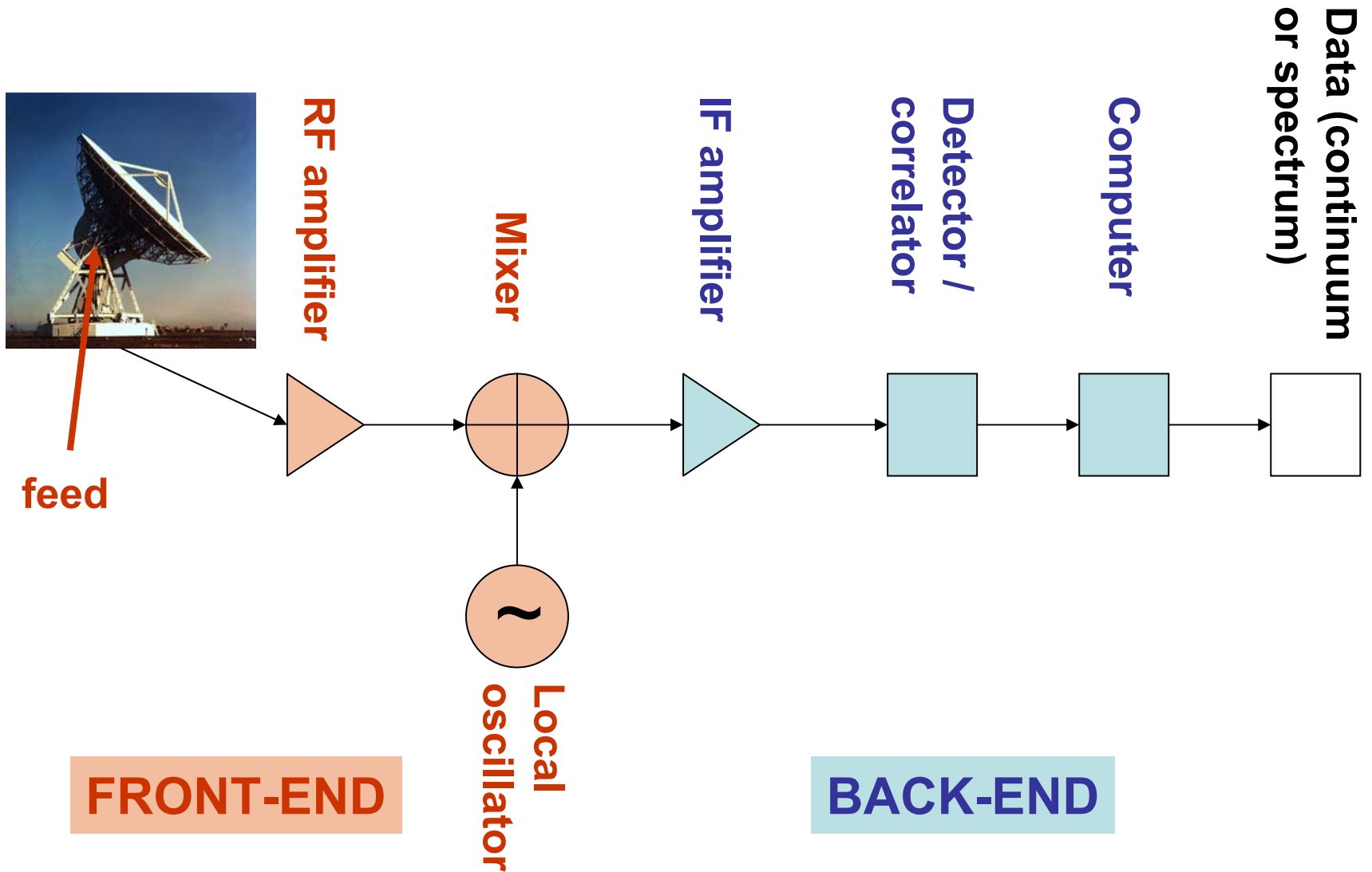
the weak signal is amplified

Antenna



A radio telescope reflects radio waves to a focus at the antenna.

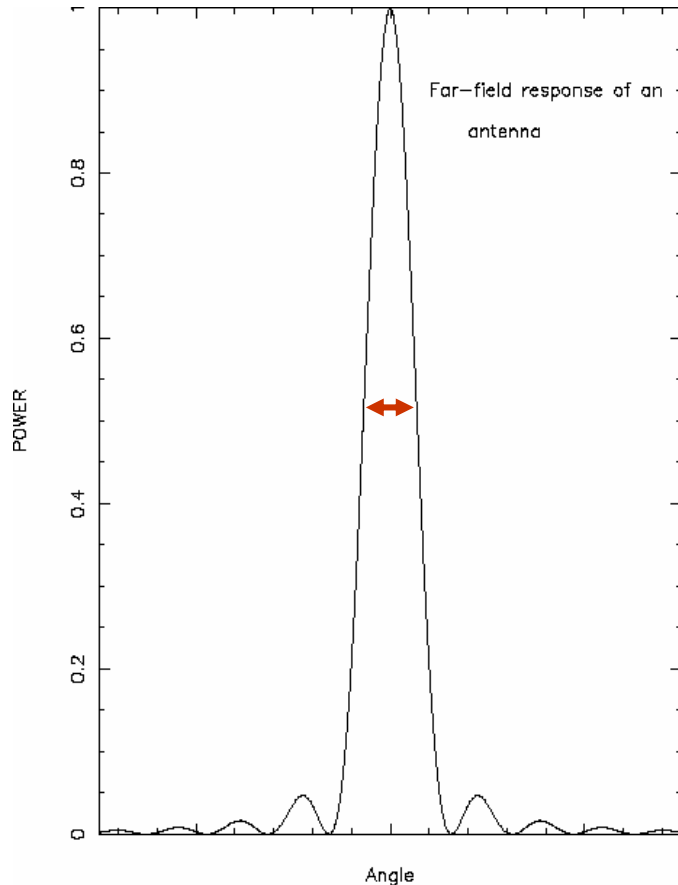
Scheme of the radio telescope instrumentation





*Medicina, IT (2004)
part of the telescope electronics*

Diffraction, beam, antenna gain



diffraction pattern
produced by the aperture

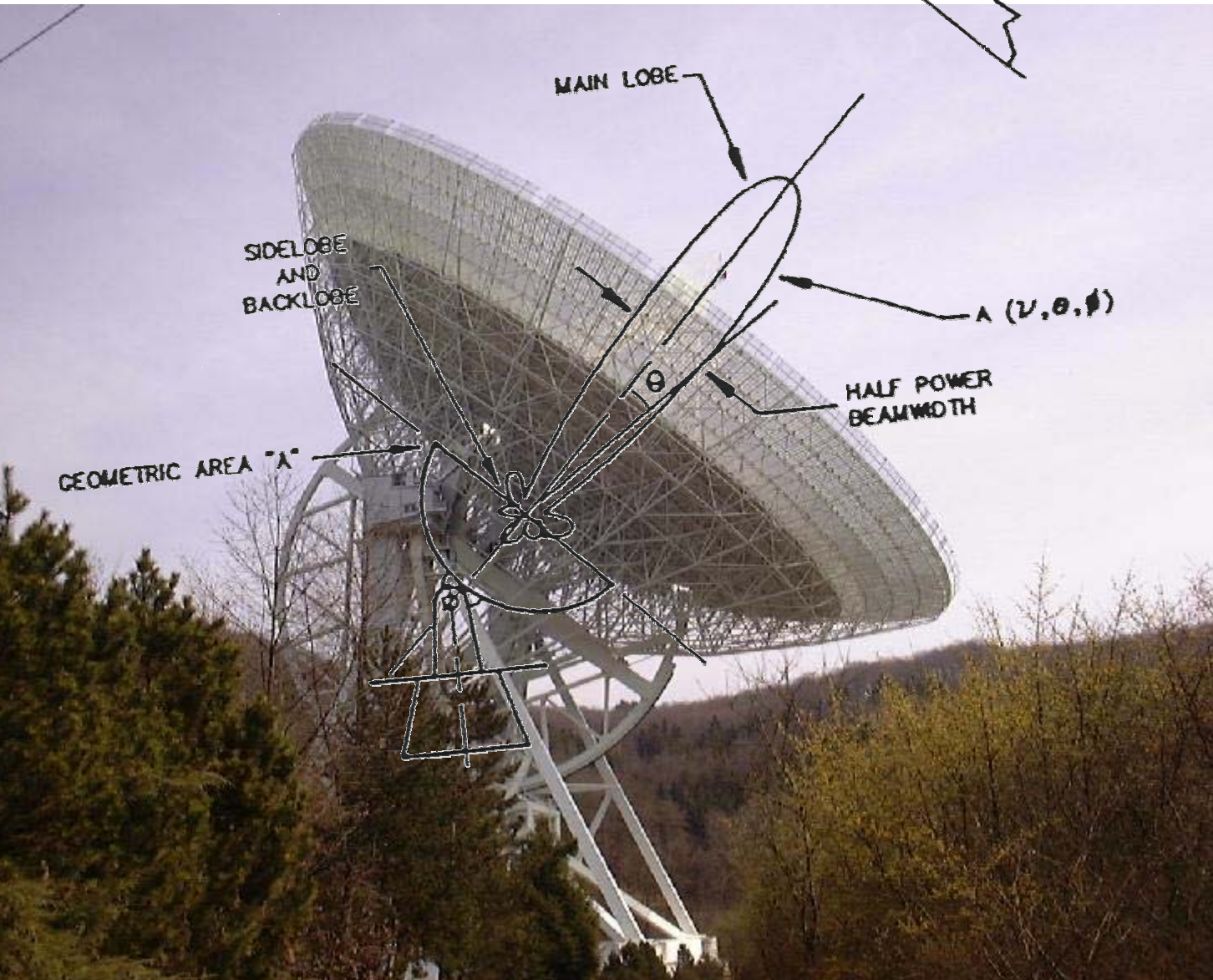
Main lobe characterised by the
half-power beamwidth

$$\theta = 1.22 \lambda / D$$

(Sidelobes are also present!)

Solid angle $\Omega = \lambda^2 / A$

Antenna gain $G = 4\pi / \Omega$



MAIN LOBE

SIDELOBE AND BACKLOBE

GEOMETRIC AREA "A"

A (ν, θ, ϕ)

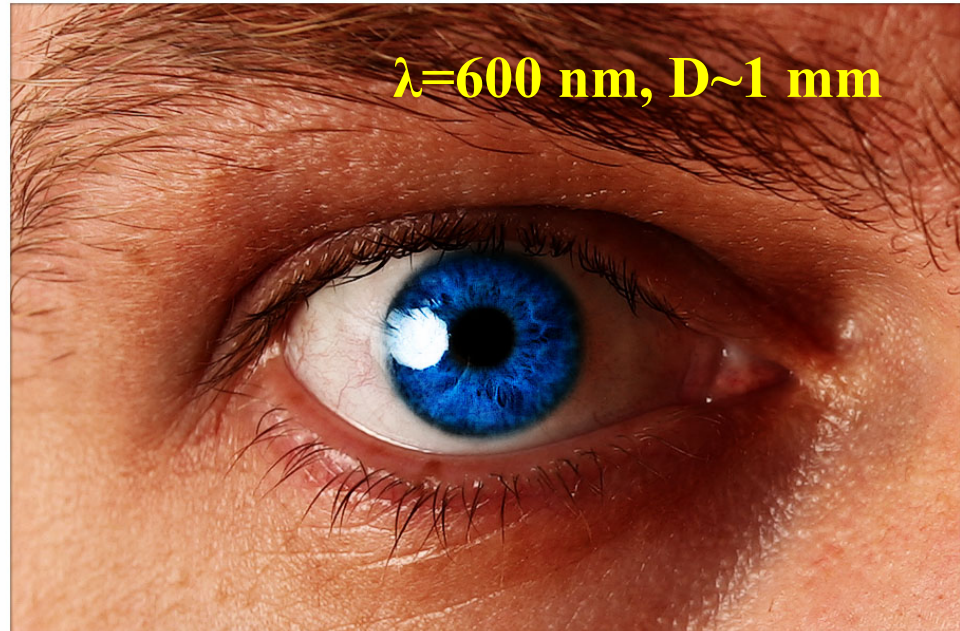
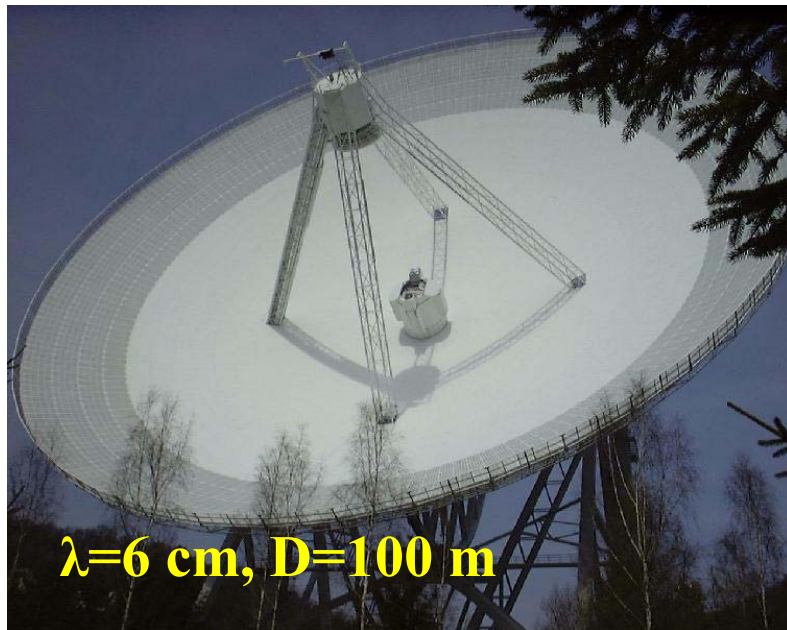
HALF POWER BEAMWIDTH

θ

Examples for angular resolution:

λ	$\theta = 1'$	$\theta = 1''$	$\theta = 1 \text{ mas}$
5 m	20 km	1 200 km	$\sim 10^6 \text{ km}$
50 cm	2 km	120 km	$\sim 10^5 \text{ km}$
5 cm	200 m	12 km	$\sim 10^4 \text{ km}$
500 nm	2 mm	12 cm	120 m

For the Hubble Space Telescope ($\lambda=500 \text{ nm}$, $D=2.4 \text{ m}$) it is $\theta \approx 50 \text{ mas}$
For the Effelsberg radio telescope ($\lambda=6 \text{ cm}$, $D=100 \text{ m}$) it is $\theta \approx 2'$



The role of radio telescope size

The power collected by a radio telescope is $P \sim S_{\nu} A \Delta\nu$

⇒ useful to have large collecting area (and large bandwidth if possible)

The angular resolution (primary beam width) is $\theta \sim \lambda / D$

⇒ larger telescopes are better in terms of resolution

However, there is a technical / financial limit at $D \approx 100$ m for constructing fully steerable dishes (Green Bank Telescope, Effelsberg)

Larger radio telescopes are either non-steerable (Arecibo: $D=305$ m spherical surface), or **interferometers**.



Arecibo, Puerto Rico

Interferometry

Two-slit interferometer (Young)

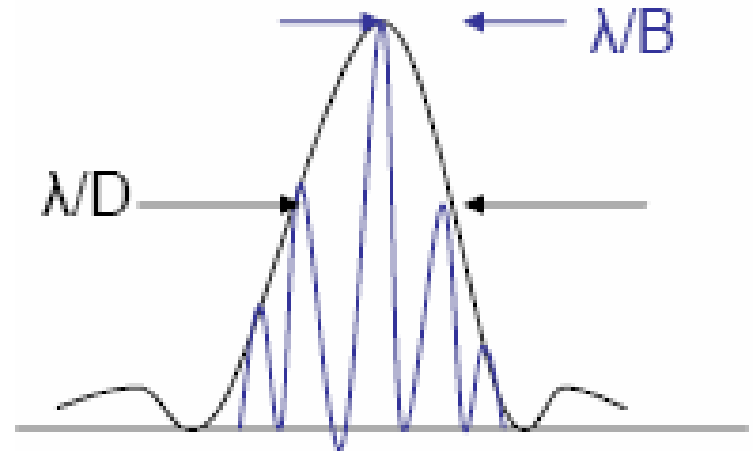
Interferometry in optical astronomy: Michelson (1891) – Jupiter's moons

Two light rays are combined in a telescope

If the star's angular extent is „small”,
the interference pattern
consist of light and dark stripes
(called *fringes*)

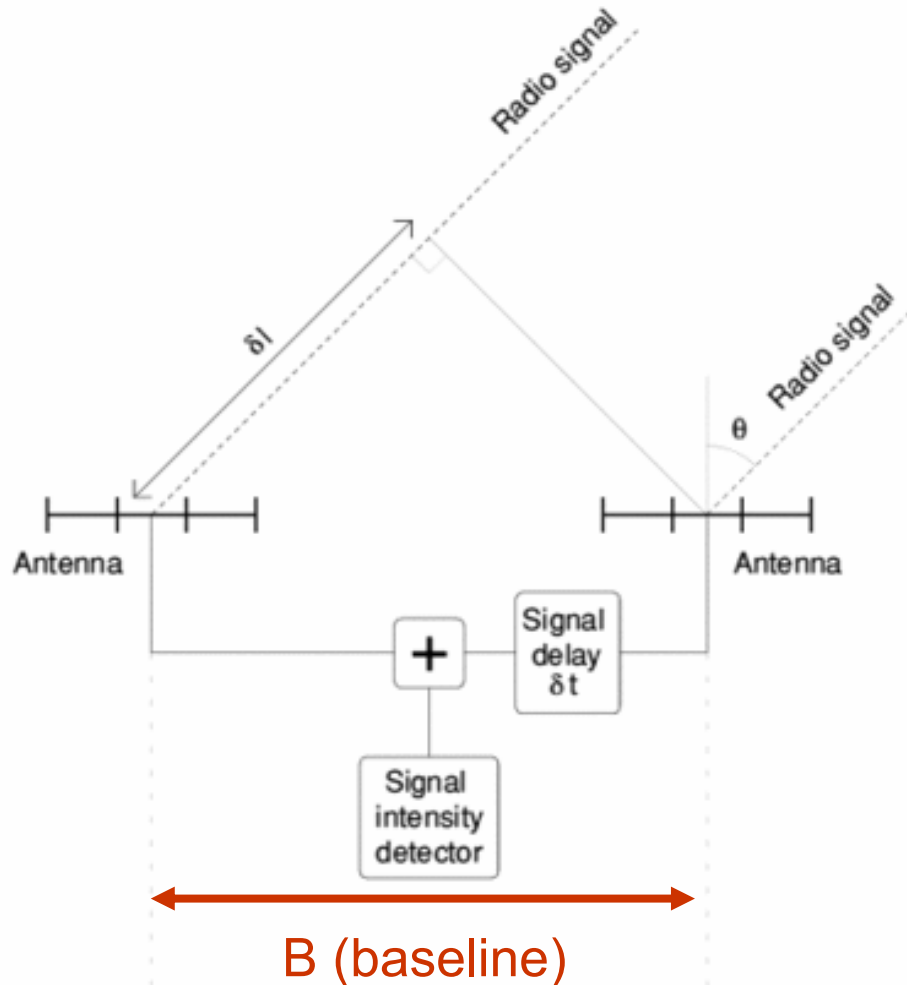
D – slit aperture diameter

B – distance between the slits



$$\text{fringe visibility} = \frac{\text{brightness of maxima} - \text{brightness of minima}}{\text{brightness of maxima} + \text{brightness of minima}}$$

Scheme of a two-element radio interferometer



As the source passes (e.g. due to the Earth rotation), the delay between the times when the wavefront reaches the two antennas changes.

The angular resolution will become

$$\theta \sim \lambda / B$$

Radio interferometry: milestones

Sea interferometer (Australia, 1946)

Jodrell Bank Interferometer (UK, 1958)

One-Mile Telescope (UK, 1963)

Green Bank Interferometer (USA, 1964)

Very Long Baseline Interferometry (VLBI) (USA, Canada, 1967)

Westerbork Synthesis Radio Telescope (The Netherlands, 1974)

Very Large Array (VLA) (USA, 1978)

Australia Telescope Compact Array (1989)

Very Long Baseline Array (VLBA) (USA, 1990)

Giant Meterwave Radio Telescope (GMRT) (India, 1997)

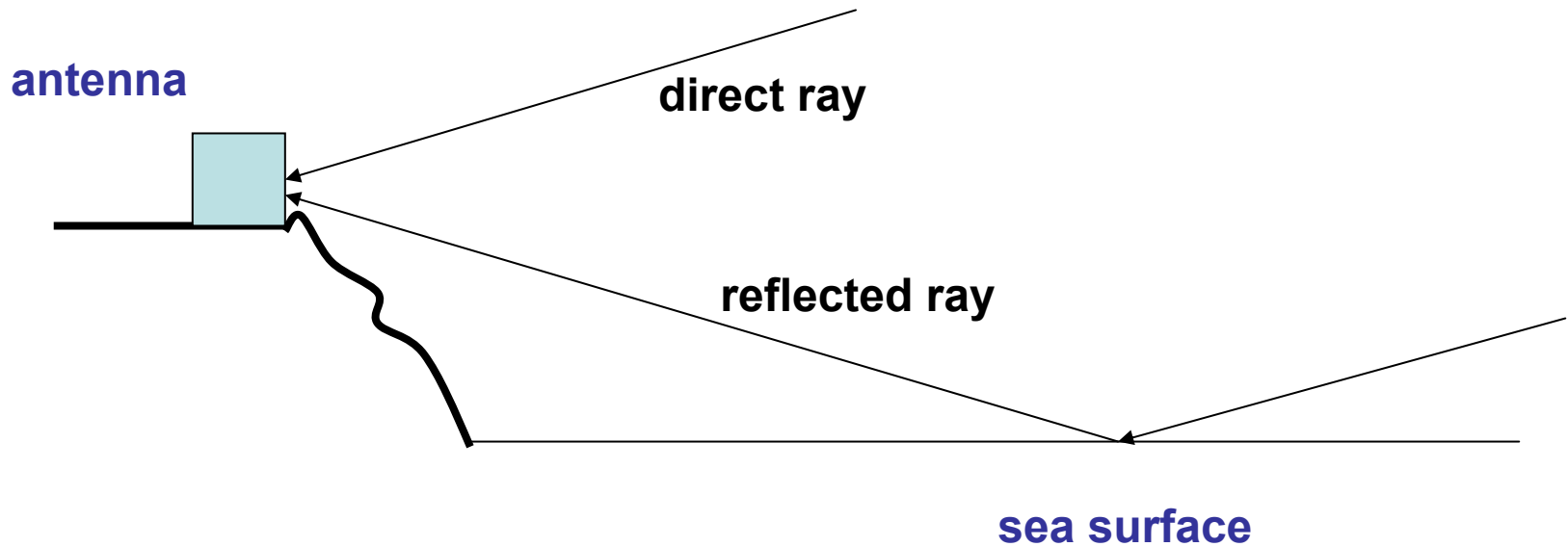
HALCA space VLBI satellite (Japan, 1997)

Radio interferometry: early history

Technique developed in Australia and the United Kingdom from the 1940's

Sea cliff interferometer (1946)

Reflection on the sea surface: phase change π + extra path length



Phase switching (Ryle, 1952)

$V_1(t)$ and $V_2(t)$ are the signal voltages from the two telescopes

Early (adding) interferometers detected $(V_1+V_2)^2$

If the phase of one signal is periodically reversed, the output is alternating between $(V_1+V_2)^2$ and $(V_1-V_2)^2$

The difference between these is $4V_1V_2$ – proportional to the time average of the cross-correlation of the two signals

Since the noise contributions of the two amplifiers are not correlated, the correlator interferometer is less sensitive to the variation in system noise

Aperture synthesis

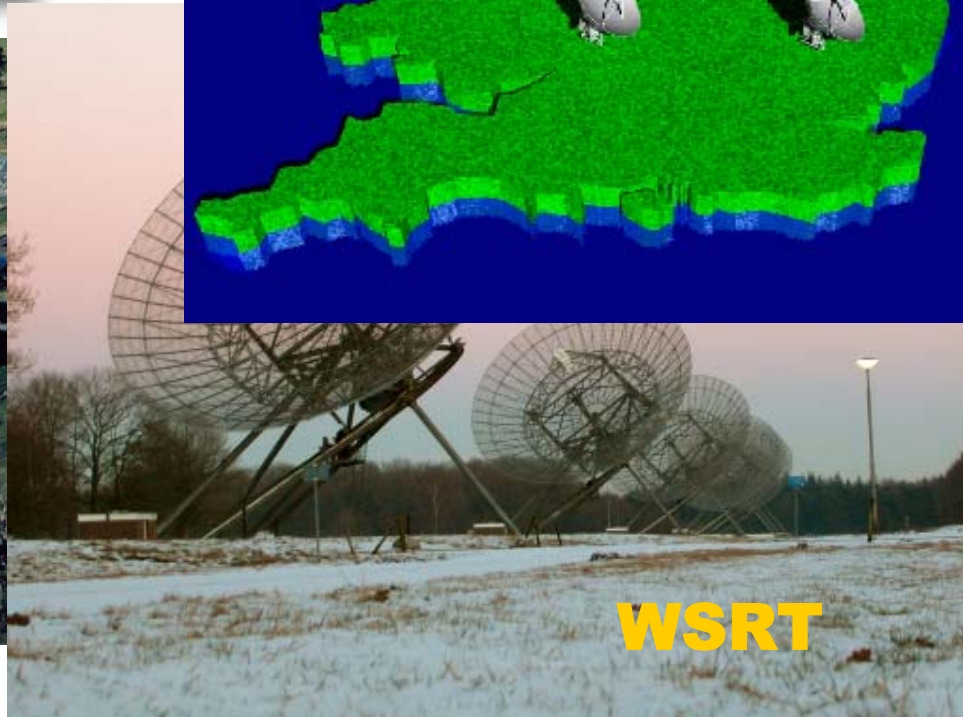
Variation of antenna baselines allow us to learn more about the radio source structure

Even with a linear array, projected baselines change as the Earth rotates, and two-dimensional visibility data can be collected for high-declination objects

The first Earth rotation synthesis instrument: *Cambridge One-Mile Telescope* (Ryle)

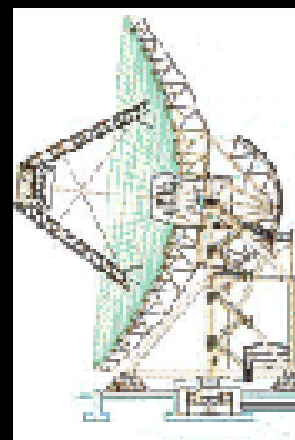
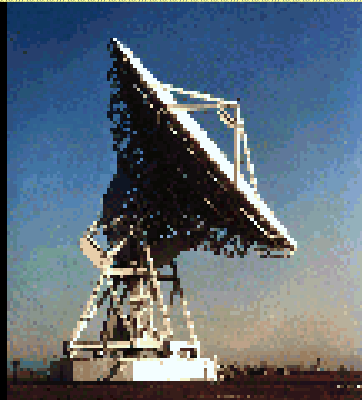
With n antennas, $n(n-1)/2$ baselines can be obtained simultaneously

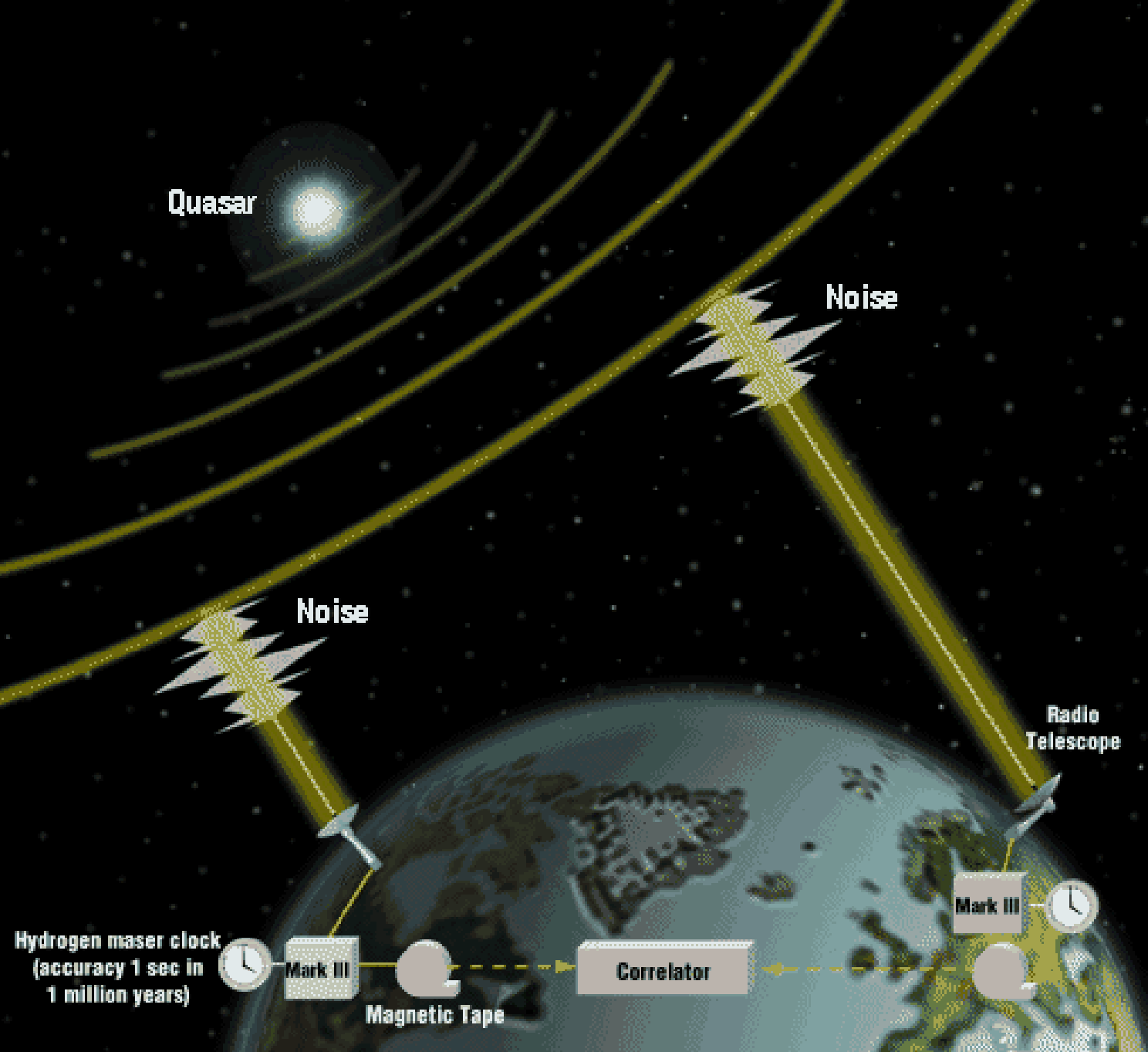
Examples of connected-element radio interferometers





Very Long Baseline Interferometry networks



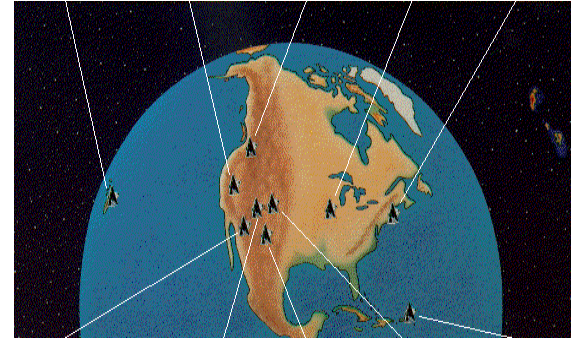


Very
Long
Baseline
Interfero
metry

VLBI facilities worldwide

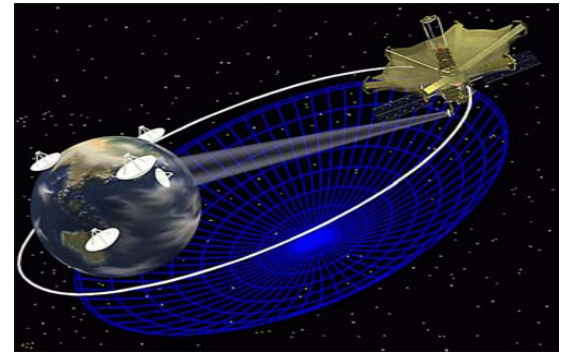
**EUROPEAN
VLBI
NETWORK**

VLBA

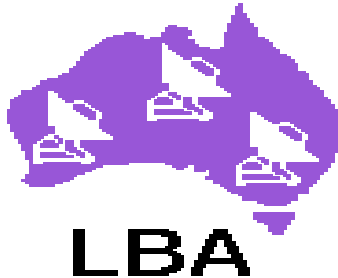


CMVA
THE COORDINATED MILLIMETER VLBI ARRAY

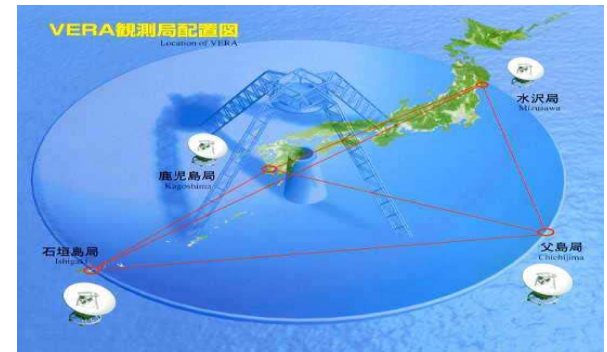
VSOP

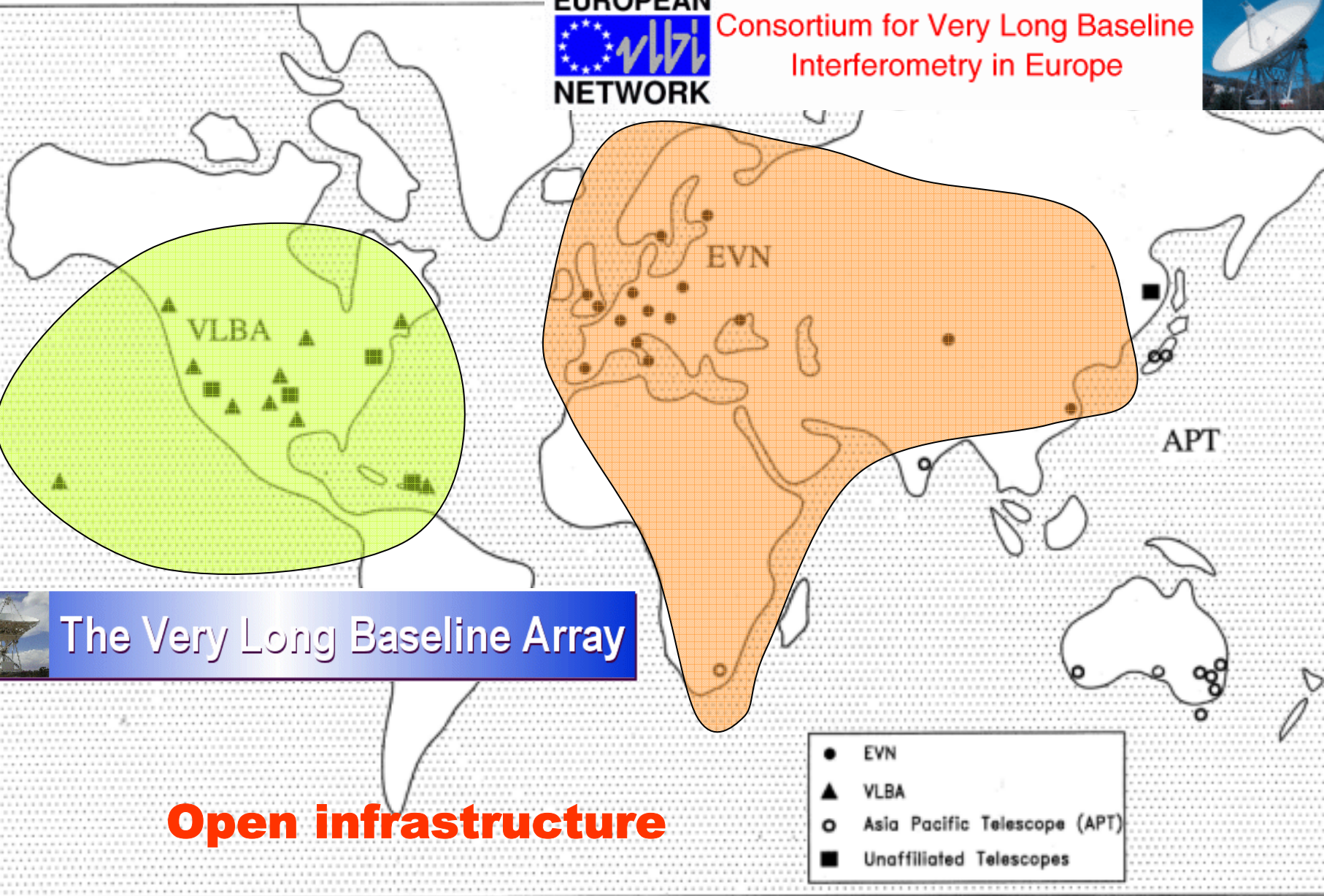


Australian LBA & APT



VERA

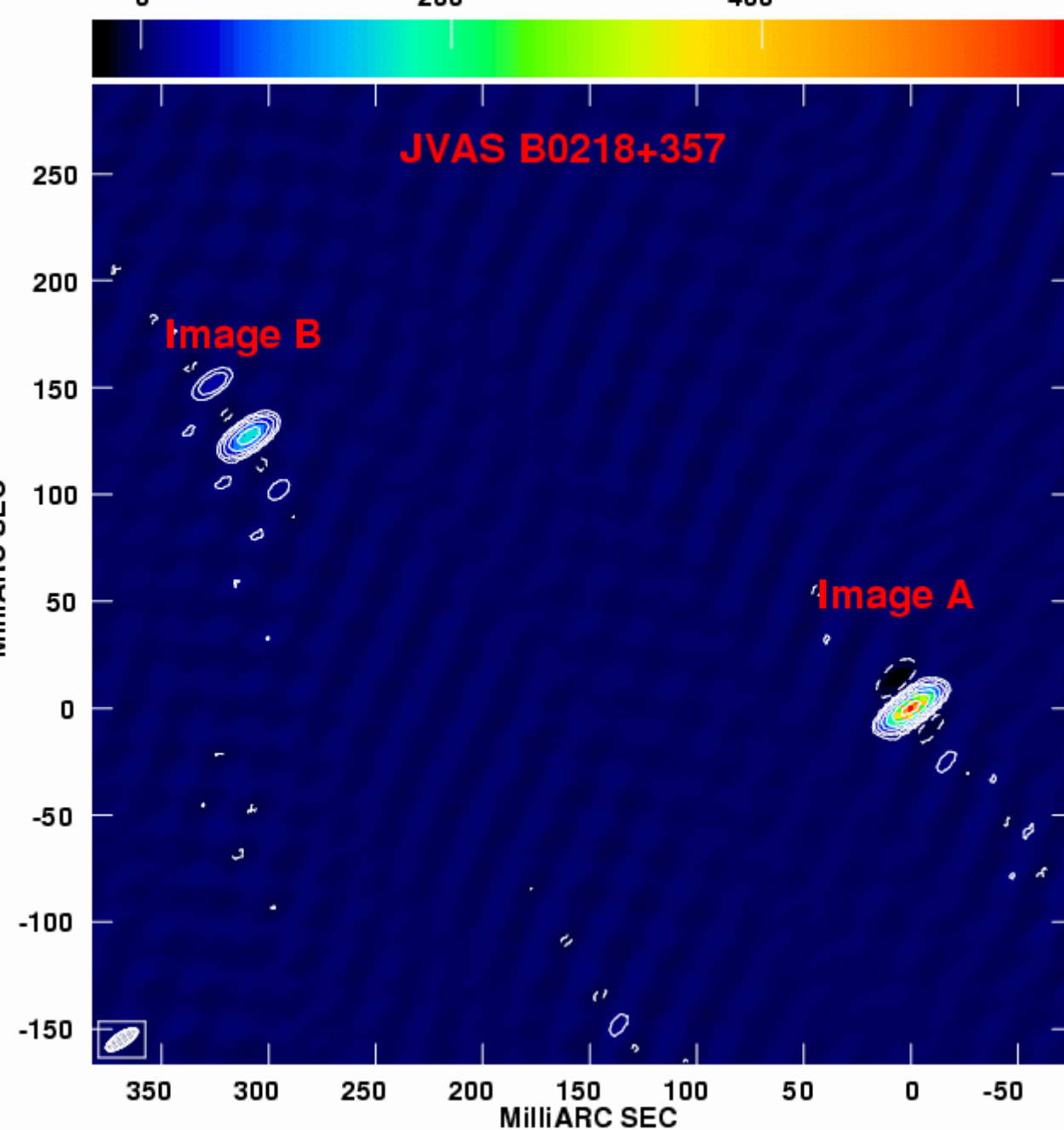




The Very Long Baseline Array

Open infrastructure

- EVN
- ▲ VLBA
- Asia Pacific Telescope (APT)
- Unaffiliated Telescopes



e-VLBI

The first real-time EVN image

28 Apr 2004

~ 2 hours

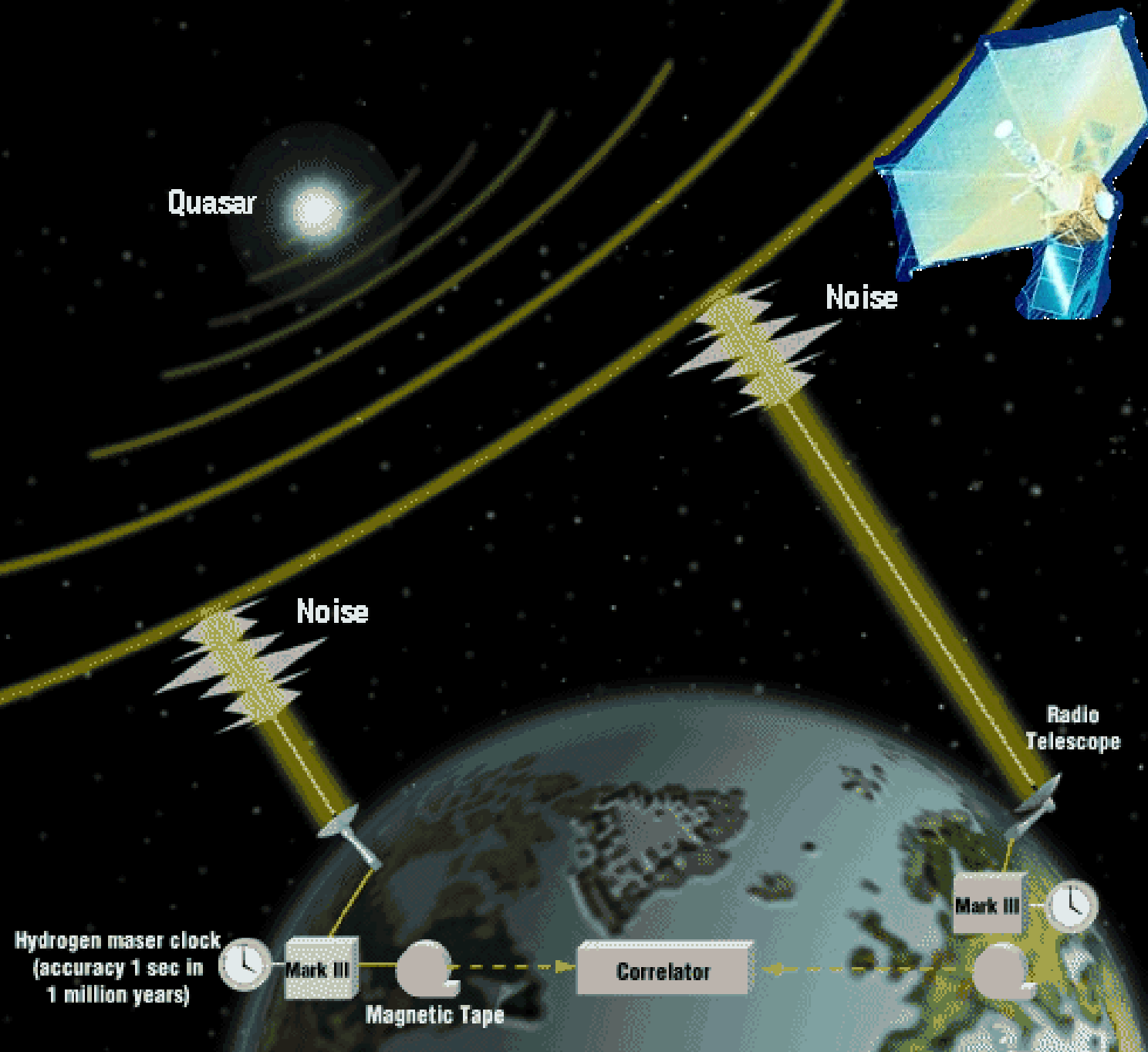
Onsala (SE),
Jodrell Bank (UK),
Westerbork (NL)

Data transfer via
optical cables to
the JIVE correlator

Data rate 32 Mbit/s

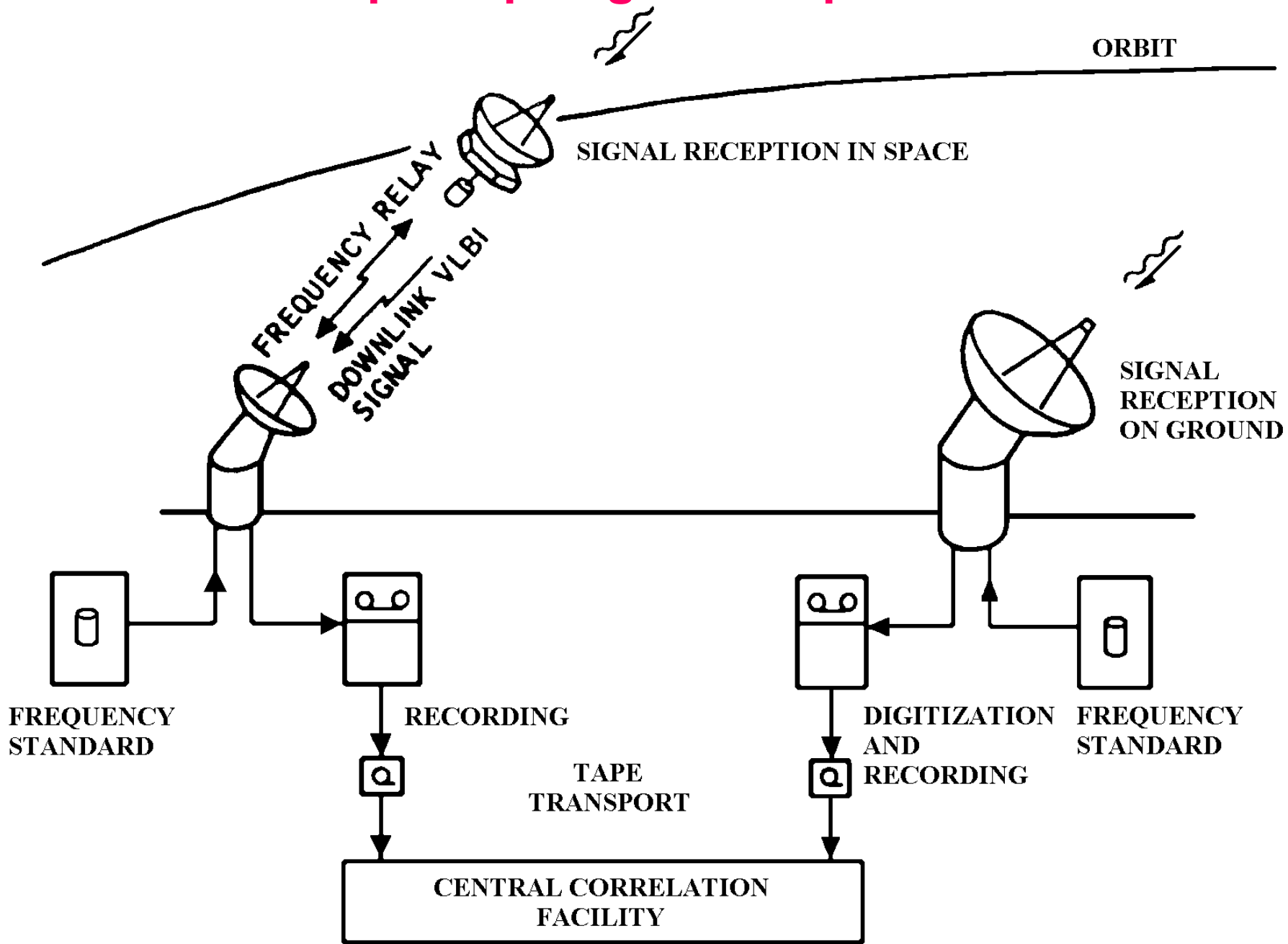


<http://www.expres-eu.org/>



Space
Very
Long
Baseline
Interfero
metry

SVLBI in principle: ground-space baseline



VSOP

(Venus and LBI Space Observatory Programme)



ISAS (Japan)

HALCA start: February 12, 1997 (new M-V rocket)

8-m parabolic antenna on board
HALCA

observing frequencies:

1.6 and 5 GHz

recording data rate: 128 Mbps

bandwidth: 32 MHz

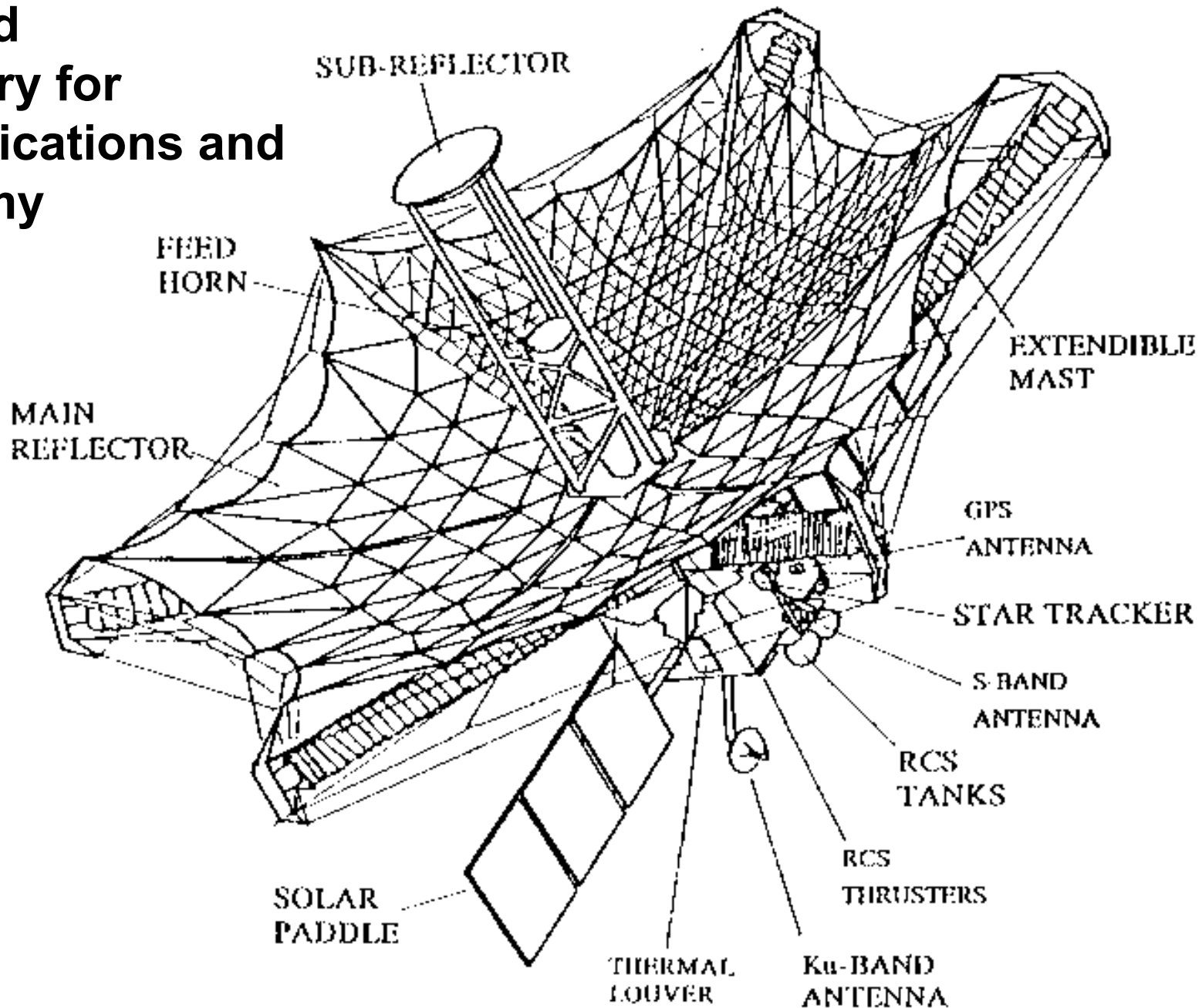
orbital period: 6.3 h

21 400km (apogee)

560 km (perigee)

baselines: up to ~30 000 km
(~3× increase in resolution)

Highly
Advanced
Laboratory for
Communications and
Astronomy



Usuda 64 m



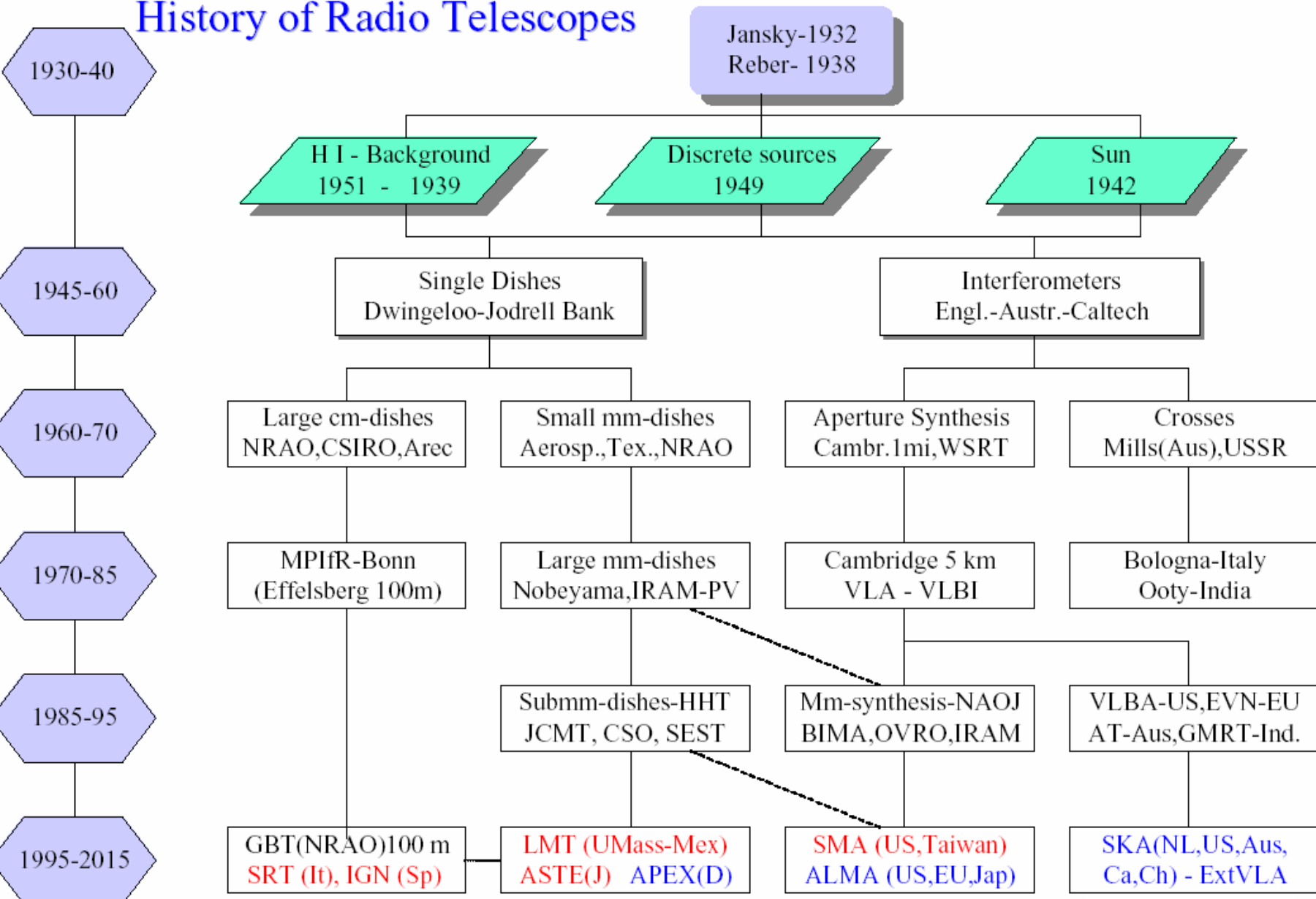
5 ground tracking stations
(USA, Japan, Australia,
Spain)

3 correlators
(USA, Canada, Japan)

a truly global VLBI:
>40 ground radio telescopes
from all over the world



History of Radio Telescopes



Optical vs. radio interferometry

In **optical** interferometers the light rays coming from the celestial source are directly interfered and produce the fringe pattern.

Radio interferometers are fundamentally different.

Here the incoming radiation is mixed with the local oscillator signals.

This method allows amplification, digitization, storage, transportation and correlation with signals coming from other telescopes.

Wavelengths are much longer in radio (factors of 10^3 - 10^6)

→ **handicap** (*from the point of view of single-telescope resolution...*)

But: **baselines** in radio can be much larger (> Earth diameter, SVLBI)

→ **best resolution in astronomy** (sub-mas)

Atmosphere: less severe in radio

atmospheric coherence scale > antenna size

variation time scale ~min (radio) vs. ms (optical)

→ phases can be calibrated in radio (with nearby compact source)

Science highlights (VLBI)

Astrophysics

- active galactic nuclei, imaging the close vicinity of supermassive BHs
- masers (galactic and extragalactic)
- radio stars, supernovae
- microquasar jets

Astrometry

- definition and densification of the celestial reference frame (ICRF)

Geodesy/geophysics

- terrestrial reference frame
- Earth orientation and rotation (the length of day)
- tectonic plate motion

Space science

- Spacecraft tracking (Huygens, SMART-1)

Interferometric imaging: some theory

Recommended reading:

Clark B.G. (1995): Interferometers and Coherence Theory, *ASP Conf. Ser.* 83, p. 3

(on-line: <http://www.cv.nrao.edu/vlbabook/clark.ps.gz>)

Cornwell T. (1995): Imaging Concepts, *ASP Conf. Ser.* 83, p. 39

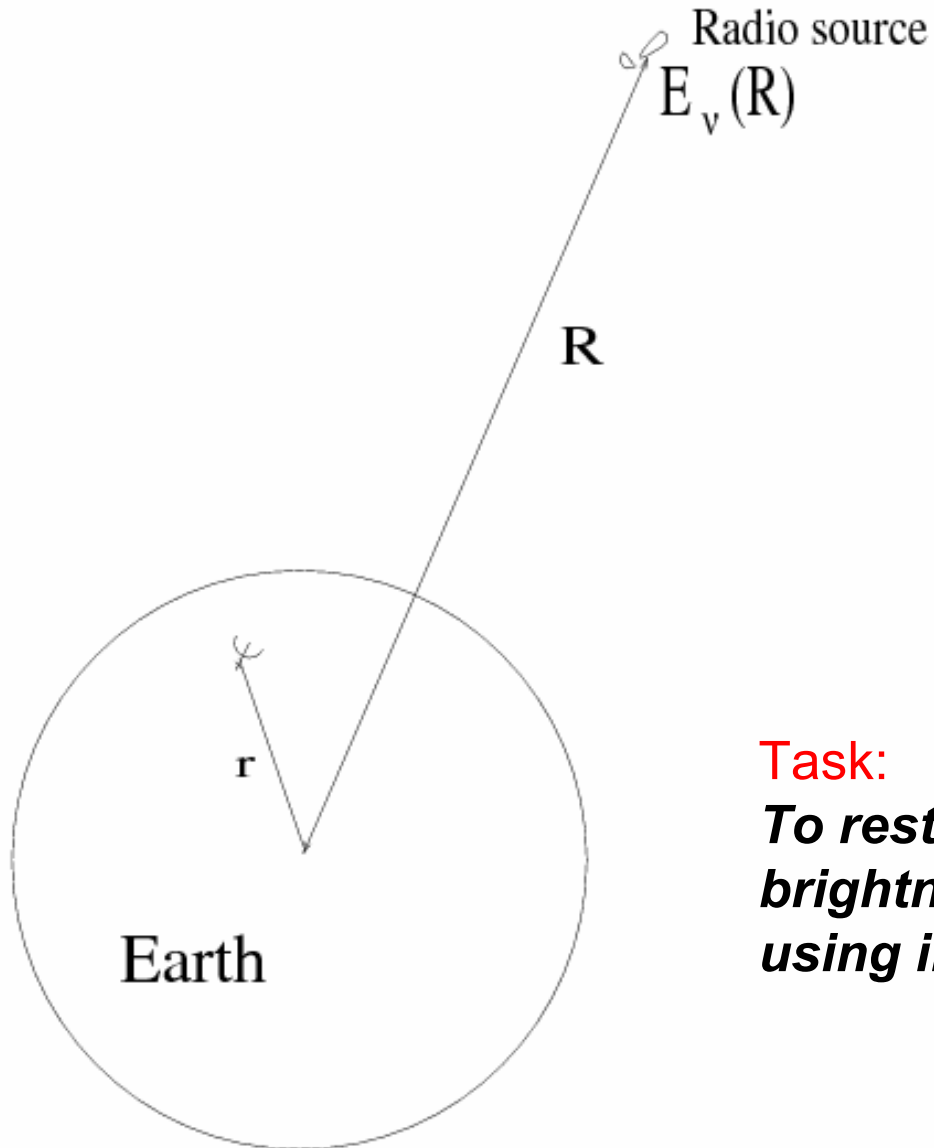
(on-line: <http://www.cv.nrao.edu/vlbabook/cornwell.ps.gz>)

Jackson N.J. (2006): Principles of interferometry

(on-line: <http://www.jb.man.ac.uk/~njj/int.ps.gz>)

Thompson A.R., Moran J.R., Swenson G.W., Jr. (1986): *Interferometry and Synthesis in Radio Astronomy* (New York: Wiley; reprints: Malabar: Krieger)

(for the more serious)



Task:
*To restore the radio source
brightness distribution on the sky,
using interferometric visibility data*

The fundamental equations of aperture synthesis *(from Clark 1995)*

$$\mathbf{E}_\nu(\mathbf{r}) = \int_{\text{source}} P_\nu(\mathbf{R}, \mathbf{r}) \mathbf{E}_\nu(\mathbf{R}) dS$$

P describes how the electromagnetic radiation propagates through the space between the source at \mathbf{R} and the antenna at \mathbf{r}

Simplified for an empty space:

$$\mathbf{E}_\nu(\mathbf{r}) = \int \frac{\mathbf{E}(\mathbf{R}) e^{2\pi i \nu |\mathbf{R} - \mathbf{r}| / c}}{|\mathbf{R} - \mathbf{r}|} dS$$

the quasi-monochromatic component of the time-varying electric field

The correlation of the field at two different observer locations \mathbf{r}_1 and \mathbf{r}_2 (i.e. two ends of an interferometer):

$$\mathbf{V}_\nu(\mathbf{r}_1, \mathbf{r}_2) = \langle \mathbf{E}_\nu(\mathbf{r}_1) \mathbf{E}_\nu^*(\mathbf{r}_2) \rangle$$

After a reasonable assumption that the radiation from two different points of the source is uncorrelated, we get

$$\mathbf{V}_\nu(\mathbf{r}_1, \mathbf{r}_2) = \int \langle |\mathbf{E}(\mathbf{R})|^2 \rangle |\mathbf{R}|^2 \frac{e^{2\pi i \nu |\mathbf{R} - \mathbf{r}_1|/c}}{|\mathbf{R} - \mathbf{r}_1|} \frac{e^{-2\pi i \nu |\mathbf{R} - \mathbf{r}_2|/c}}{|\mathbf{R} - \mathbf{r}_2|} dS$$

If $\mathbf{R} \gg \mathbf{r}$ (the far-field condition), then

$$|\mathbf{R} - \mathbf{r}| = \sqrt{|\mathbf{R}|^2 + |\mathbf{r}|^2 - 2\mathbf{r} \cdot \mathbf{R}} \approx |\mathbf{R}| - \frac{\mathbf{r} \cdot \mathbf{R}}{|\mathbf{R}|}$$

Further simplifications to make the life easier:

- ignore the vector nature of \mathbf{V}
- introduce the intensity of the radiation field $I = |\mathbf{R}|^2 \langle |\mathbf{E}_\nu| \rangle^2$
- use the unit vector \mathbf{s} pointing to the direction of \mathbf{R}
- integrate over the solid angle subtended by the radio source

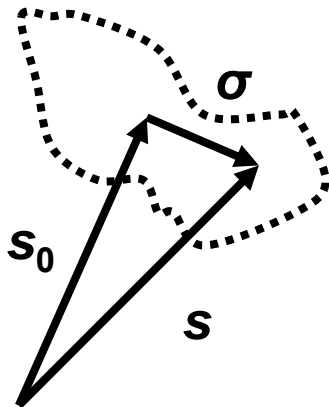
$$V_\nu(\mathbf{r}_1, \mathbf{r}_2) = \int I_\nu(\mathbf{s}) e^{-2\pi i \nu \mathbf{s} \cdot (\mathbf{r}_1 - \mathbf{r}_2) / c} d\Omega$$

V is the spatial coherence function

Important note: it depends on $\mathbf{r}_1 - \mathbf{r}_2$ only, i.e. one end of the baseline can be moved into an arbitrary location

Under certain conditions, V is invertible, and the intensity distribution of the source can be reconstructed.

Let's introduce a special coordinate system:



$$\mathbf{s} = \mathbf{s}_0 + \boldsymbol{\sigma}$$

the source is "small" $\rightarrow \mathbf{s}_0 \perp \boldsymbol{\sigma}$

$$\mathbf{s}_0 = (0, 0, 1) \quad \textit{phase center}$$

$$\mathbf{s} = (x, y, 1)$$

The coordinates of the baseline vector $\mathbf{r}_1 - \mathbf{r}_2$ in this system are

$$\mathbf{r}_1 - \mathbf{r}_2 = c/v (u, v, w) = \lambda (u, v, w)$$

We can now rewrite the spatial coherence function with the (x, y) sky coordinates and the (u, v) coordinates:

$$V_\nu(\mathbf{r}_1, \mathbf{r}_2) = \int I_\nu(\mathbf{s}) e^{-2\pi i \nu \mathbf{s} \cdot (\mathbf{r}_1 - \mathbf{r}_2) / c} d\Omega$$

$$V_\nu(u, v, \cancel{w}) = \cancel{e^{-2\pi i w}} \iint I_\nu(x, y) e^{-2\pi i (ux + vy)} dx dy$$

Fourier-transform, may be formally inverted:

$$I_\nu(x, y) = \iint V_\nu(u, v) e^{2\pi i (ux + vy)} du dv$$

In practice, the spatial coherence function is (by far) not sampled everywhere in the (u, v) plane – i.e. our hypothetical aperture is not filled (*see coverage plots later*)

Instead, we have a sampling function $S(u, v)$, of which the possible values are 1 or 0, if measurements are taken or not

$$I_\nu^D(x, y) = \iint V_\nu(u, v) S(u, v) e^{2\pi i(ux+vy)} du dv$$

This is called **dirty image** in the radio interferometry jargon

$$I_\nu^D = I_\nu * B, \quad \text{where} \quad B(x, y) = \iint S(u, v) e^{2\pi i(ux+vy)} du dv$$

is the **dirty beam** or, in other words, the interferometer's response to a point source (PSF)

In practical imaging, the sampling function $S(u, v)$ is coupled with some form of data weighting

$$S(u, v) = \sum_k w_k \delta(u - u_k) \delta(v - v_k)$$

For example, *natural weighting* uses some power (-2 or sometimes -1) of the noise associated with the k -th data point (optimal for image noise level):

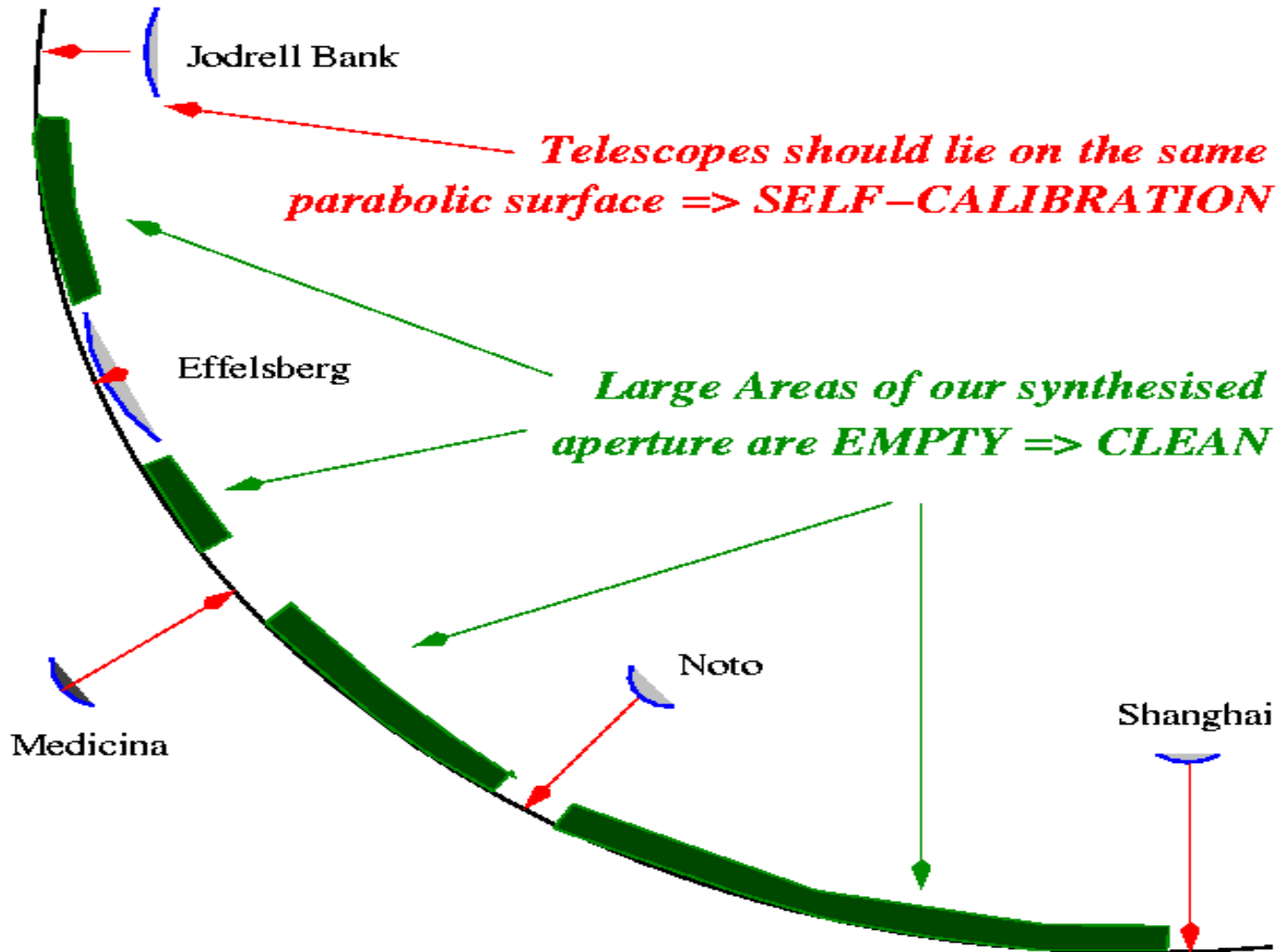
$$w_k = \frac{1}{\sigma_k^2}$$

In *uniform weighting*, the weight attached to a visibility point is inversely proportional to the local density of the data points in the (u, v) plane (optimal for high angular resolution):

$$w_k = \frac{1}{\rho(u_k, v_k)}$$

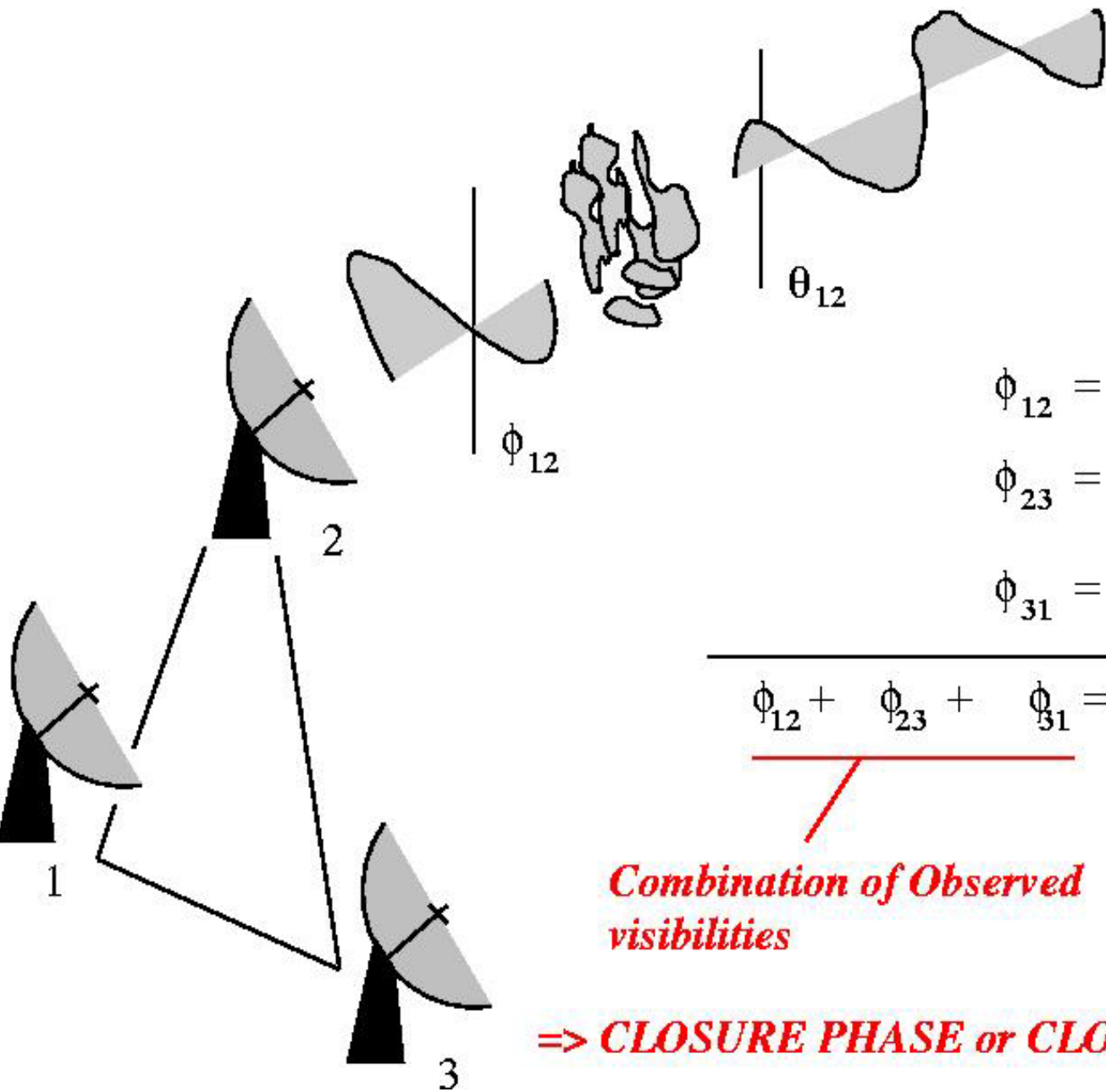
Task: to synthesise a giant radio telescope from small antennas

- Earth rotation helps to fill in the (u,v) plane
- Computational “tricks” are needed to restore the source brightness distribution on the sky (i.e. to make an image of the source)



Trick #1: Self-calibration

- Path length of radiation from the radio source to the telescope is not constant, e.g. phase errors are introduced via atmosphere above telescopes, clock errors, etc.
- For an array of N telescopes we measure (instantaneously) $N(N-1)/2$ corrupted interferometer measurements
- ***self-calibration*** is based on understanding that the corrupted visibilities mostly arise from telescope-based errors – and there are only N of these
- it is possible to solve for these N errors by using combinations of the corrupted visibilities (closure quantities) AND an assumed model of the source (***hybrid mapping***, see later...)



$$\phi_{12} = \theta_{12} + \phi_1 - \phi_2$$

$$\phi_{23} = \theta_{23} + \phi_2 - \phi_3$$

$$\phi_{31} = \theta_{31} + \phi_3 - \phi_1$$

$$\phi_{12} + \phi_{23} + \phi_{31} = \theta_{12} + \theta_{23} + \theta_{31}$$

Combination of Observed visibilities

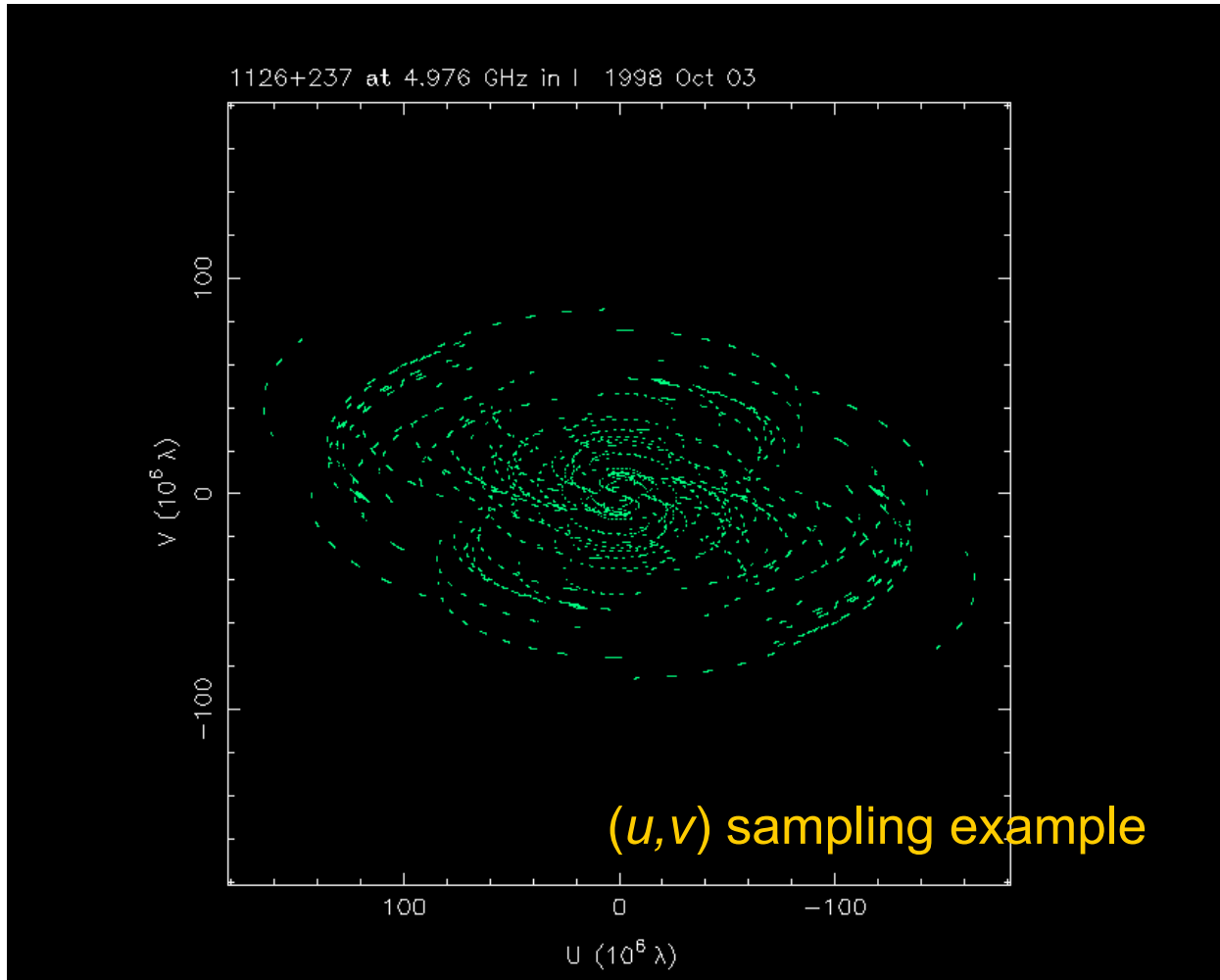
Combination of TRUE visibilities

=> CLOSURE PHASE or CLOSURE QUANTITIES

(amplitudes are multiplicative; we need min. 4 antennas for closure)

Image deconvolution

- A VLBI synthesised aperture is not filled with data (in fact mostly *empty!*)

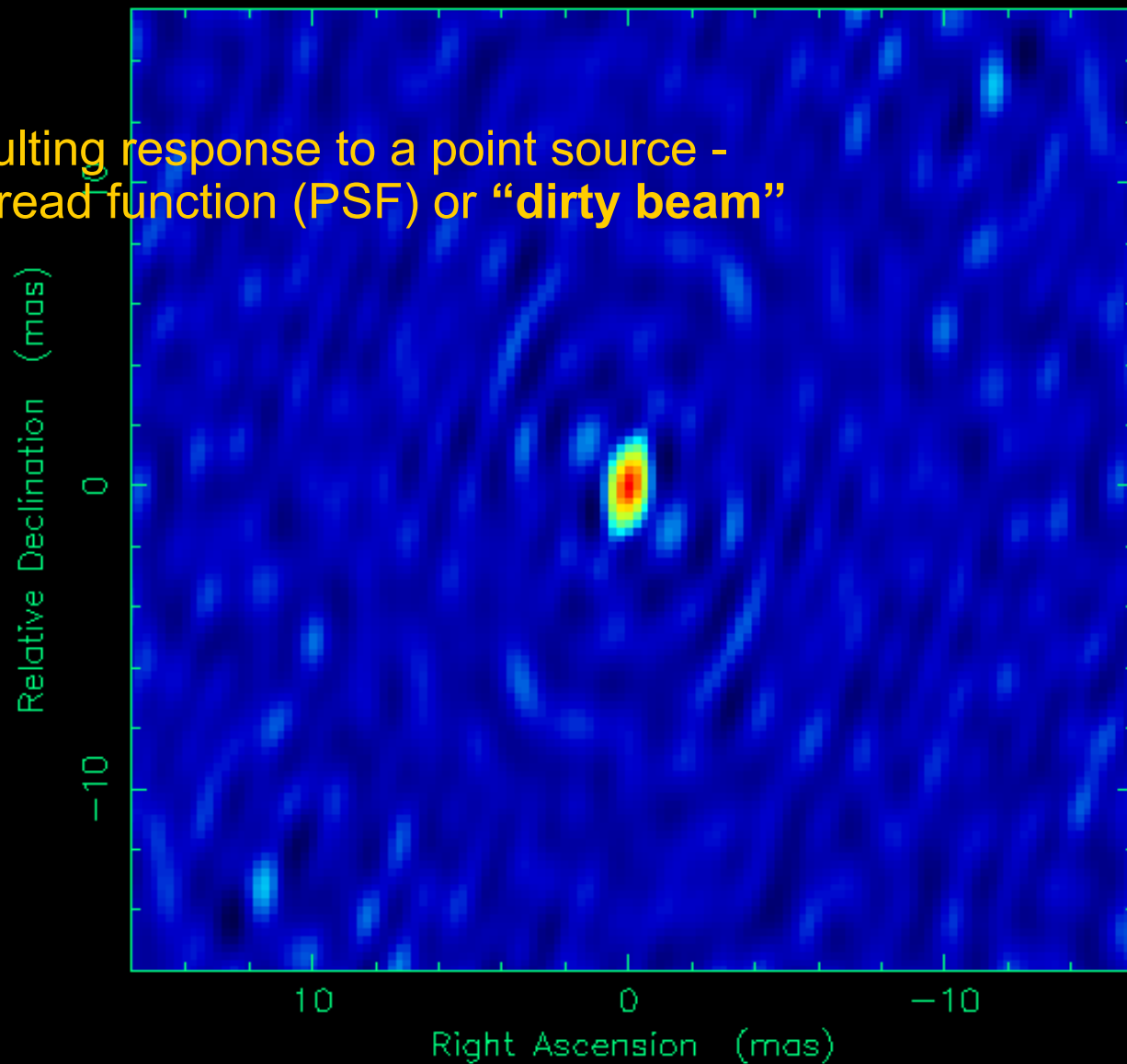


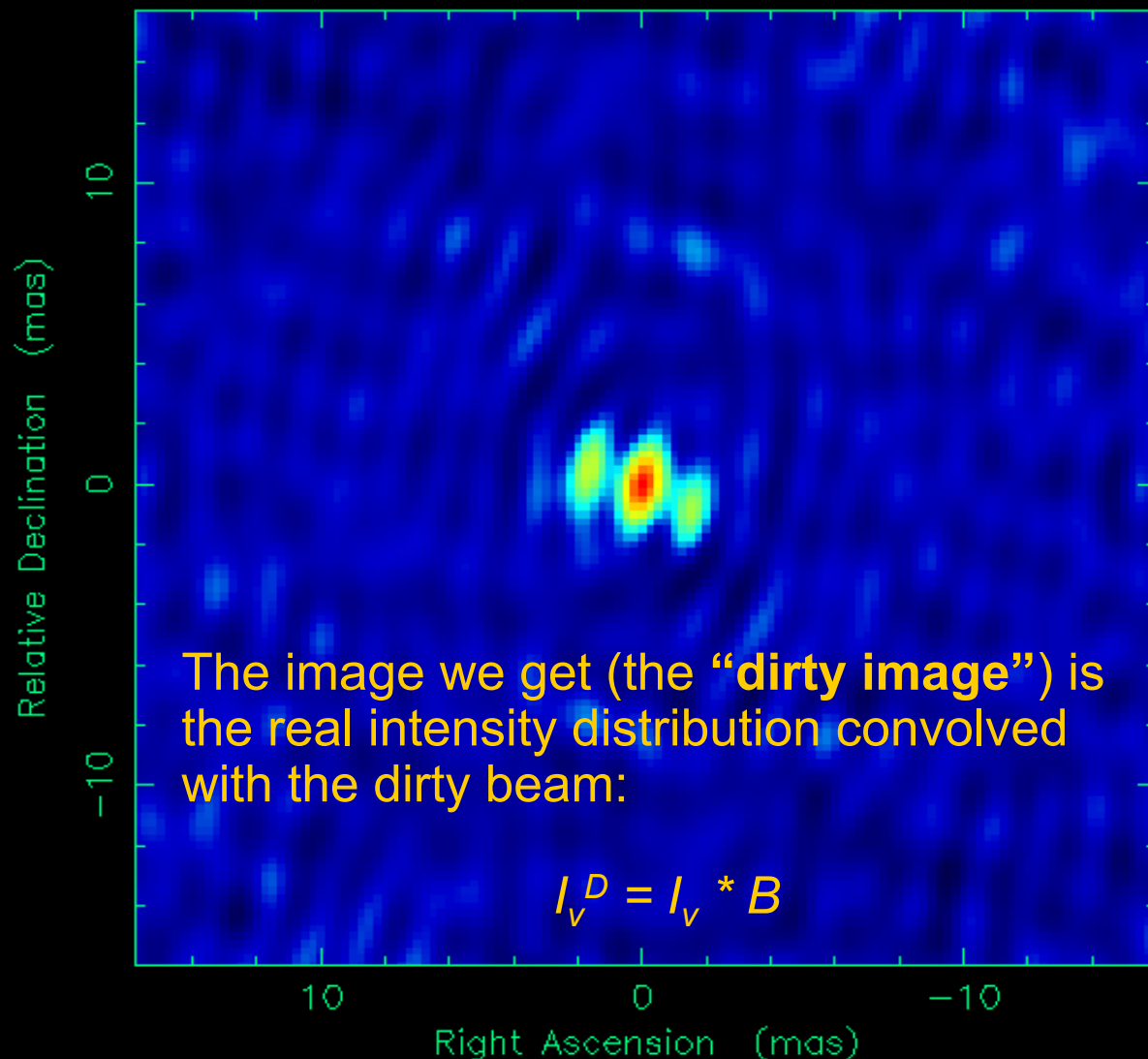
Software

*Examples shown here (and the demonstration session) are prepared with the Caltech **Difmap** difference mapping software, one of the standard VLBI imaging packages
(see: www.astro.caltech.edu/~tjp/citv1b)*

*“The” radio interferometry data reduction package is the NRAO Astronomical Image Processing System (**AIPS**), suitable for initial calibration, fringe-fitting, editing, averaging, imaging, and a lot more...
(www.aips.nrao.edu)*

The resulting response to a point source -
point spread function (PSF) or “dirty beam”





Trick #2: CLEAN algorithm

- Basic assumption: the sky brightness distribution can be decomposed into a finite number of ***point sources***
- Sequence of steps:
 - pick the brightest point in the dirty map
 - multiply the peak by the loop gain (<1)
 - subtract a point source response (dirty beam) with a flux density maximum * the loop gain from the dirty image
 - store the component's position and intensity
 - next iteration (until there is a peak above the noise level on the residual map)
- after many iterations, a CLEAN component model is built up at the end
- final image: the ***CLEAN model*** convolved with an ***“ideal” beam*** (a fitted Gaussian in practice) + the residual image is added

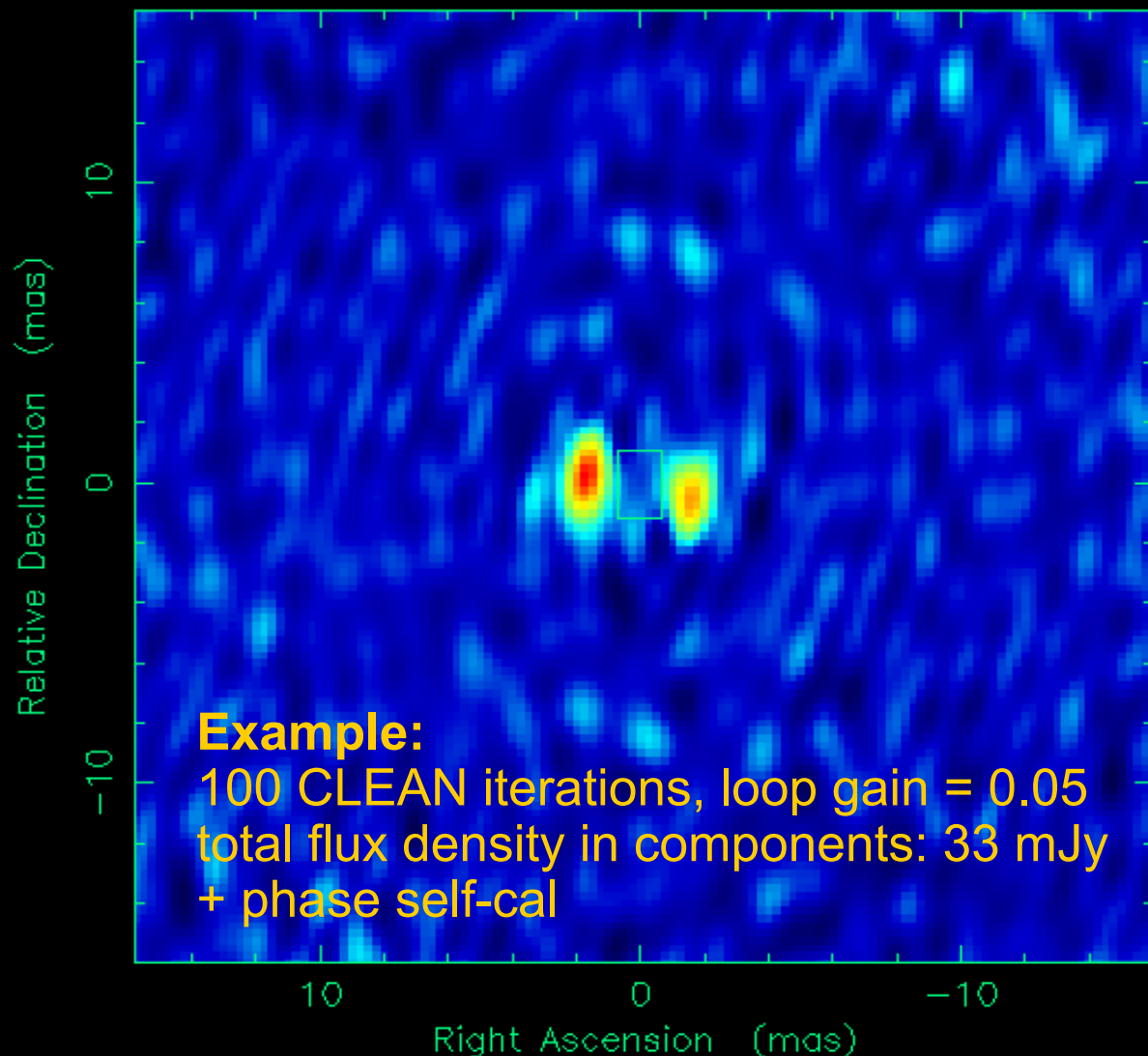
Hybrid mapping

- A combination of **deconvolution** (e.g. CLEAN) and **self-calibration**
- The CLEAN model from the previous stage is used as a source model for self-cal

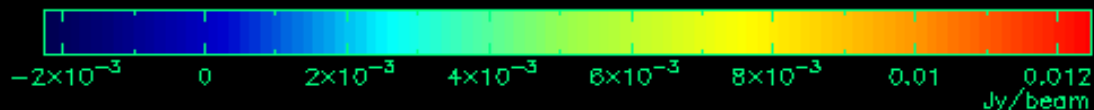
- Sequence of steps:
 - start with a simple initial source model (i.e. point)
 - predict visibilities according to the model
 - keep the observed amplitudes
 - solve for antenna-specific phase errors using the closure phases
 - correct the observed visibilities with antenna phase errors
 - form a new dirty image
 - use deconvolution (CLEAN) to obtain an improved model
 - next iteration

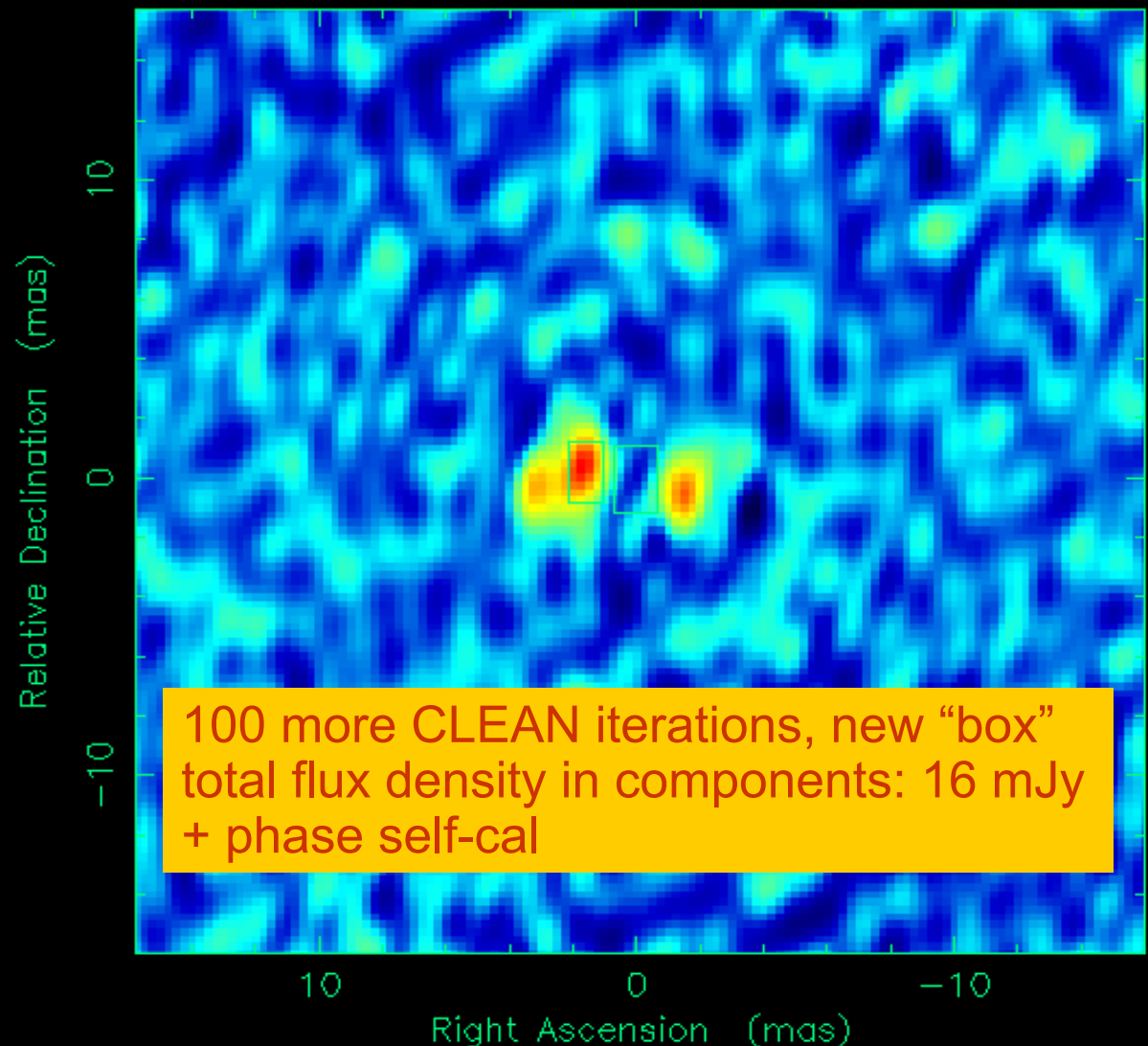
- after sufficient number of phase-only self-cal, antenna gain (amplitude) corrections can be determined gradually

- the process converges to the final image
- *a SNR of at least ~ 3 is needed within the atmospheric coherence time*



Map center: RA: 11 28 51.697, Dec: +23 26 17.240 (2000.0)
Displayed range: $-0.00227 \rightarrow 0.0125$ Jy/beam



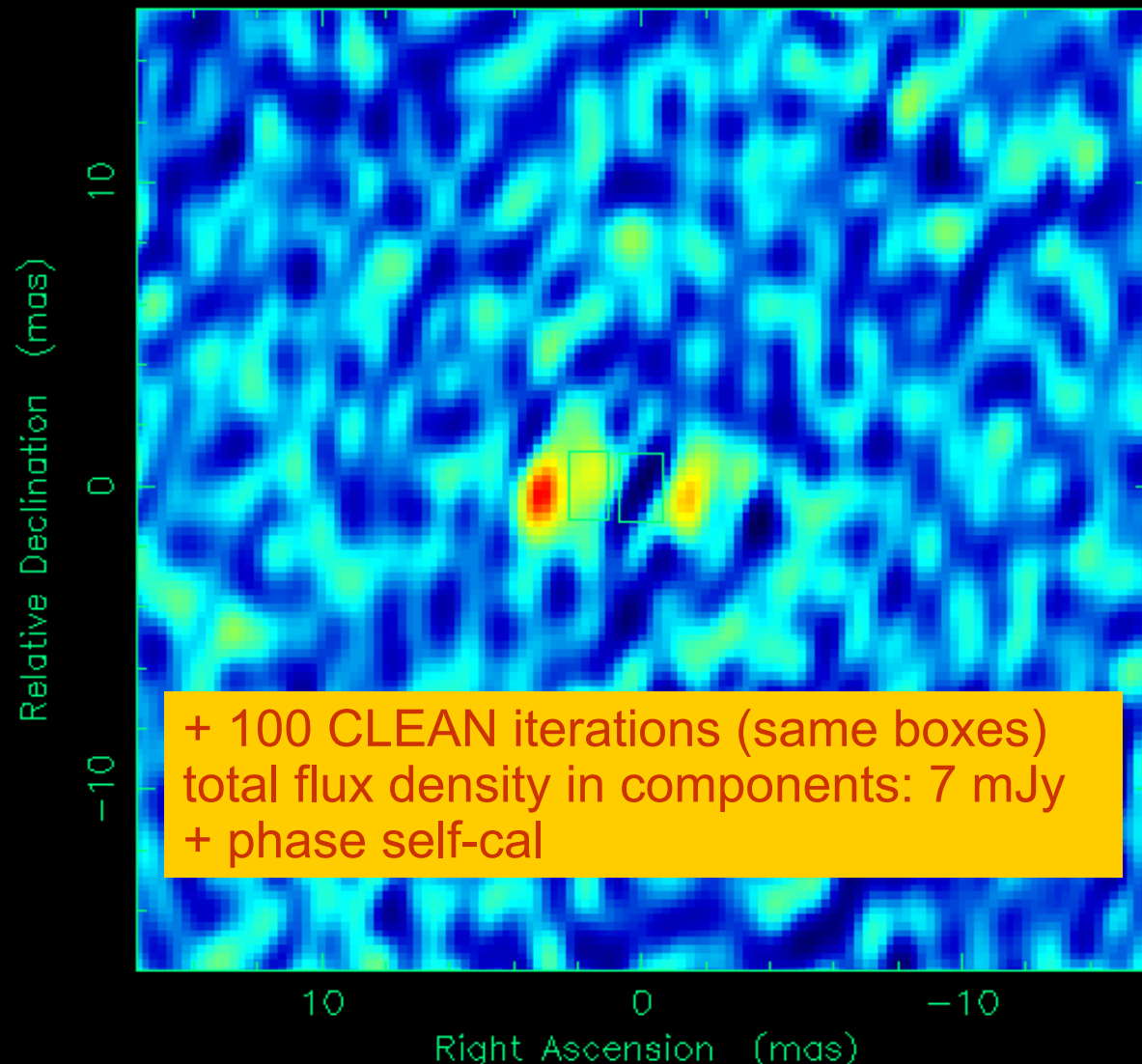


100 more CLEAN iterations, new "box"
total flux density in components: 16 mJy
+ phase self-cal

Map center: RA: 11 28 51.697, Dec: +23 26 17.240 (2000.0)
Displayed range: $-0.00176 \rightarrow 0.00525$ Jy/beam



Residual I map: Array: BEPHEKNOF3M
1126+237 at 4.976 GHz 1998 Oct 03

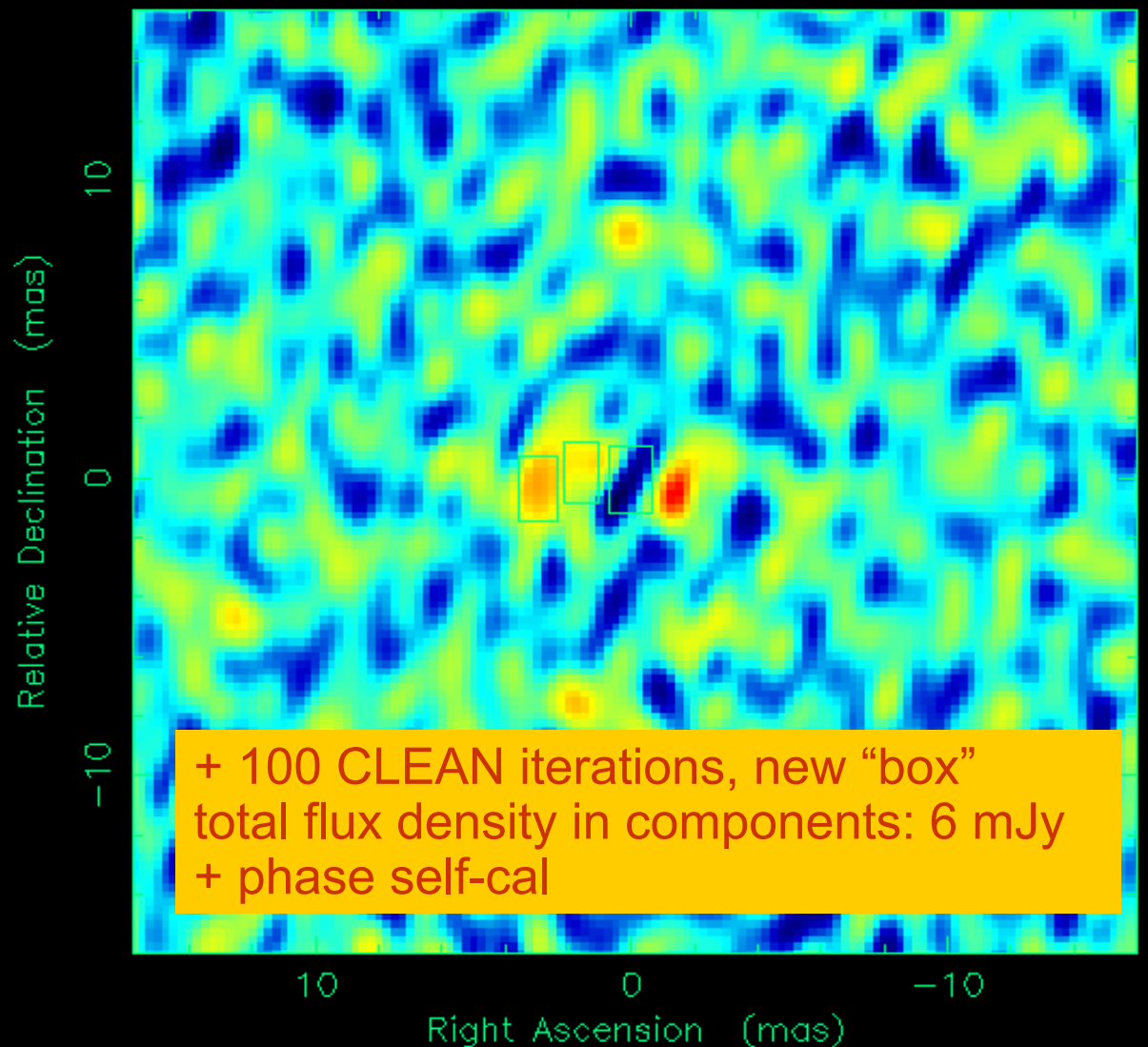


+ 100 CLEAN iterations (same boxes)
total flux density in components: 7 mJy
+ phase self-cal

Map center: RA: 11 28 51.697, Dec: +23 26 17.240 (2000.0)
Displayed range: $-0.00137 \rightarrow 0.00397$ Jy/beam



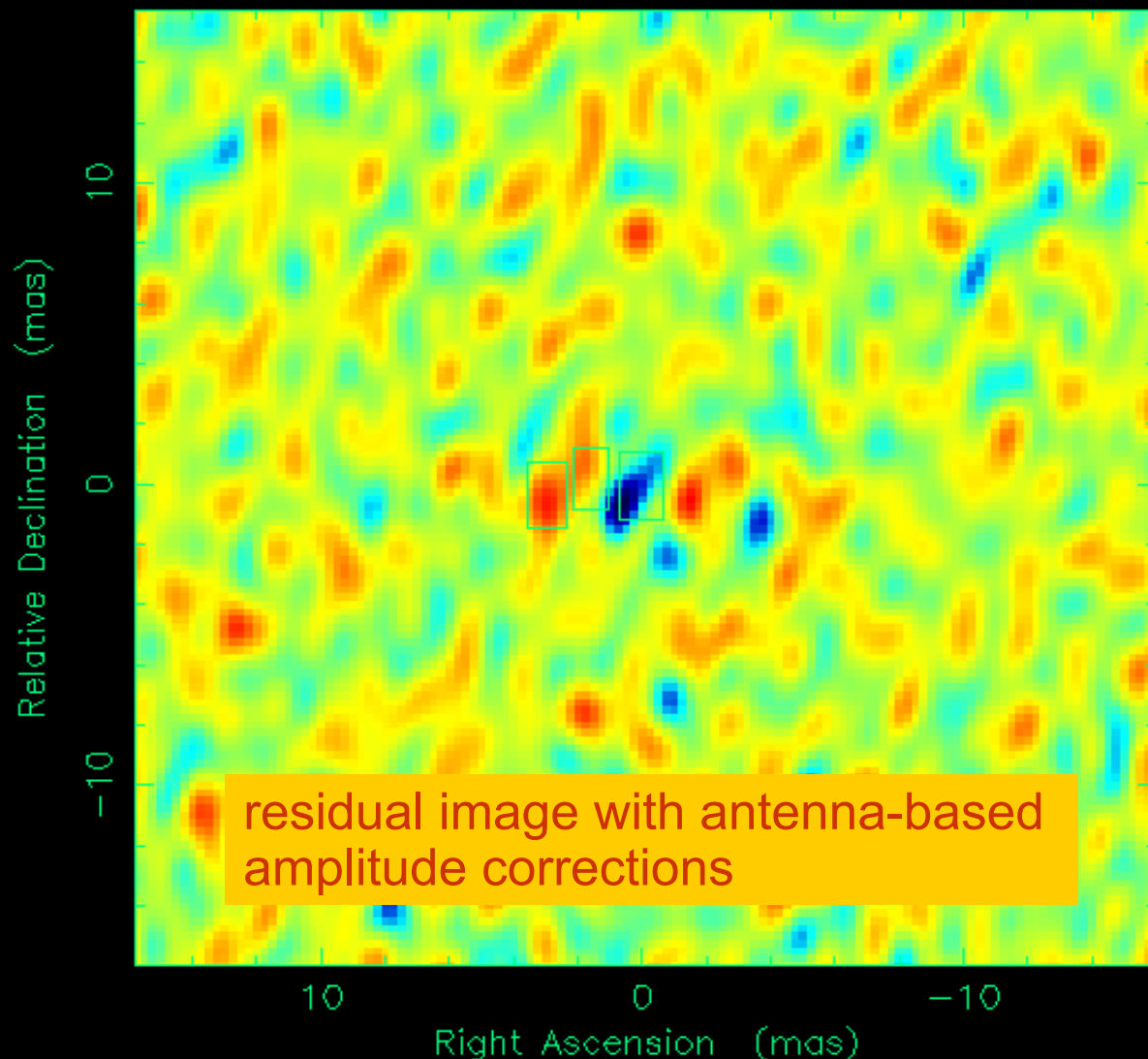
Residual I map: Array: BEFHKLNOPSM
1126+237 at 4.976 GHz 1998 Oct 03



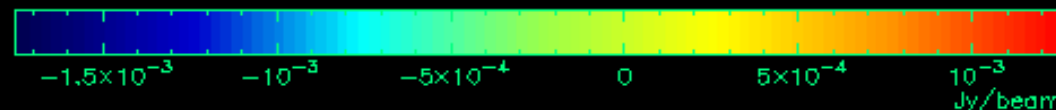
Map center: RA: 11 28 51.697, Dec: +23 26 17.240 (2000.0)
Displayed range: $-0.00115 \rightarrow 0.0021$ Jy/beam



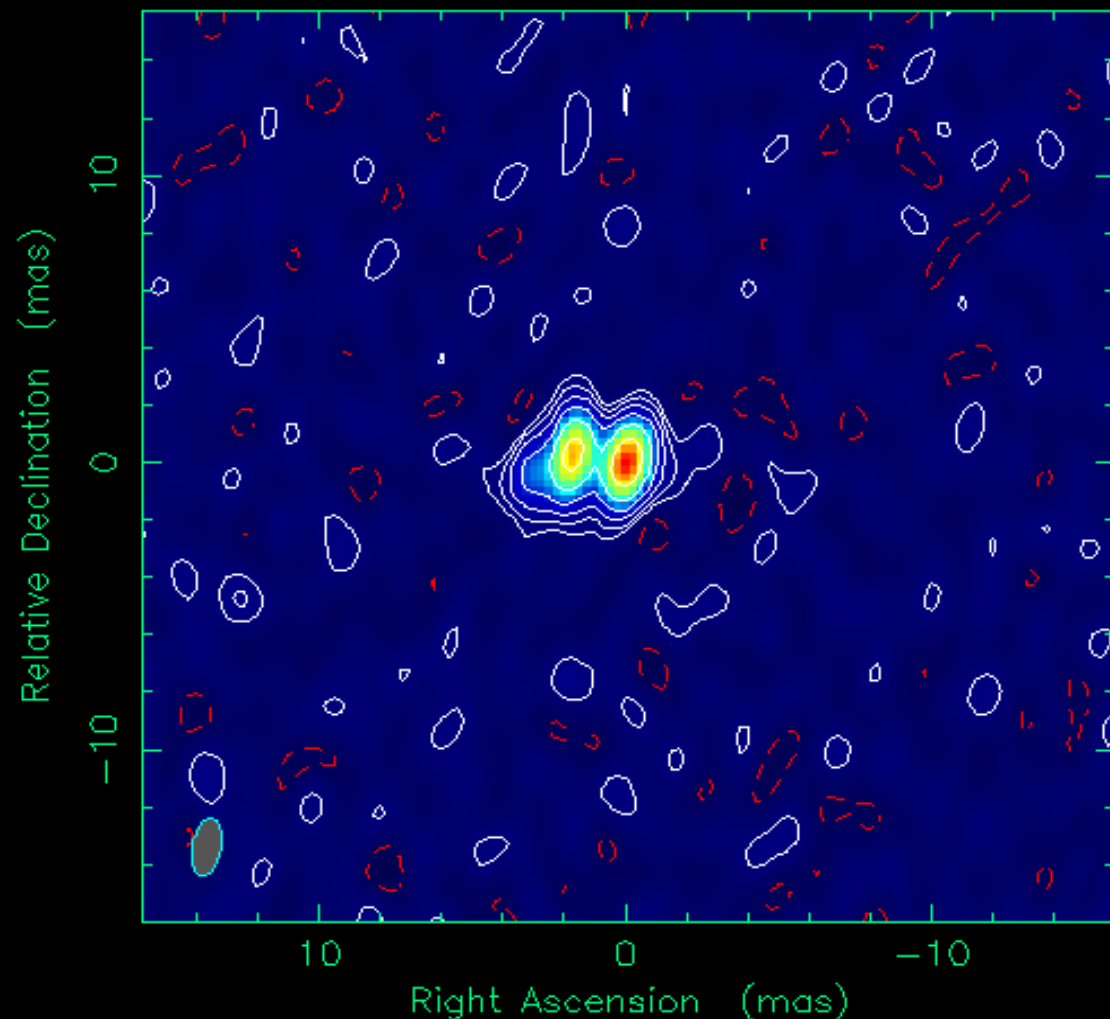
Residual I map: Array: BEPHEKNOF3M
1126+237 at 4.976 GHz 1998 Oct 03



Map center: RA: 11 28 51.697, Dec: +23 26 17.240 (2000.0)
Displayed range: $-0.00175 \rightarrow 0.00126$ Jy/beam



Clean 1 map. Array: BEPHEKNOF3M
1126+237 at 4.976 GHz 1998 Oct 03



Map center: RA: 11 28 51.697, Dec: +23 26 17.240 (2000.0)

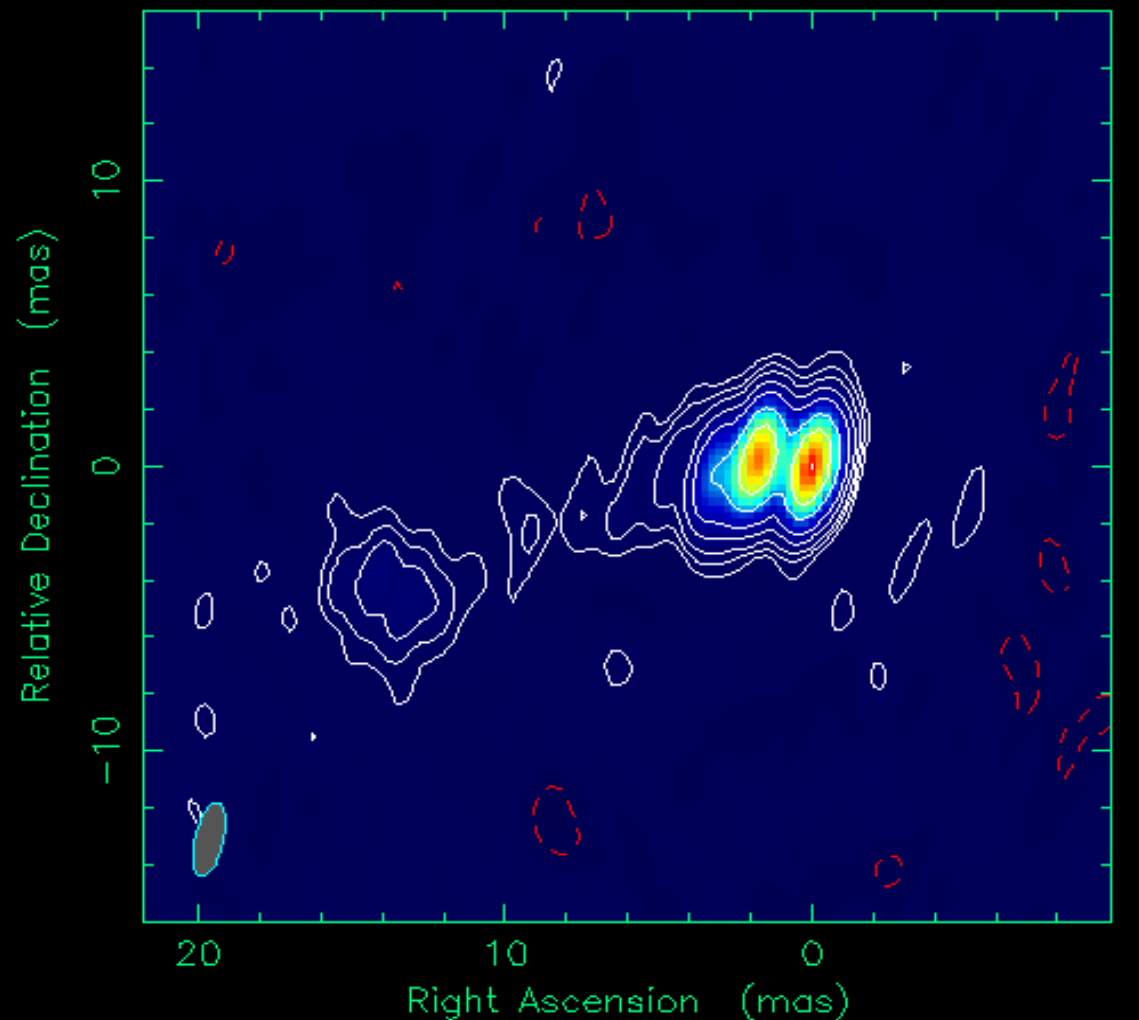
Map peak: 0.0238 Jy/beam

Contours %: -2 2 4 8 16 32 64

Beam FWHM: 2.05 x 0.941 (mas) at -9.47°



Clean 1 map. Array: BEFHKLNOPSM
1126+237 at 4.976 GHz 1998 Oct 03



Map center: RA: 11 28 51.697, Dec: +23 26 17.240 (2000.0)

Map peak: 0.0252 Jy/beam

Contours %: -0.7 0.7 1.4 2.5 5 10 25 50 99

Beam FWHM: 2.64 x 0.925 (mas) at -12°

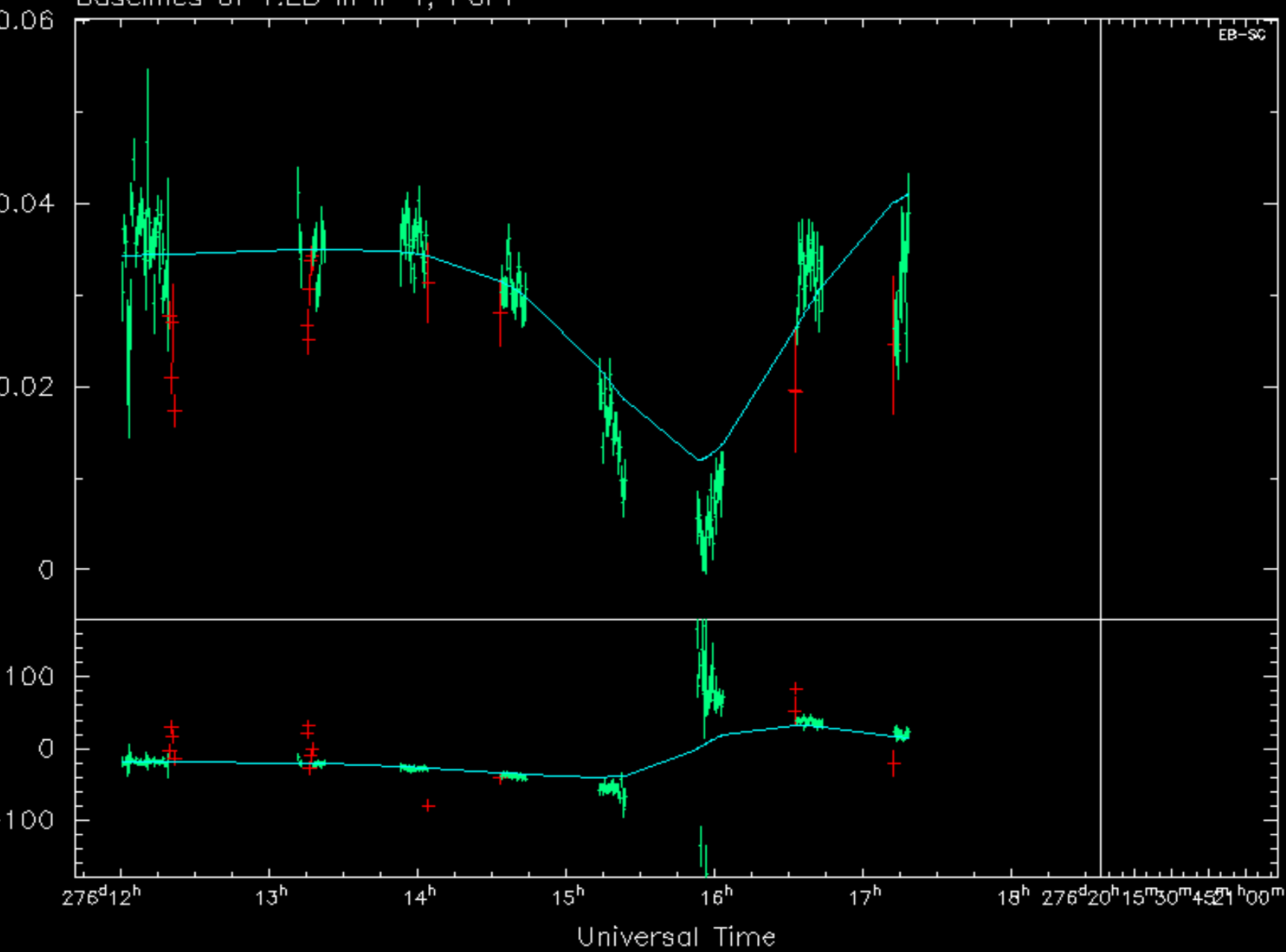


Observed vs. model visibilities

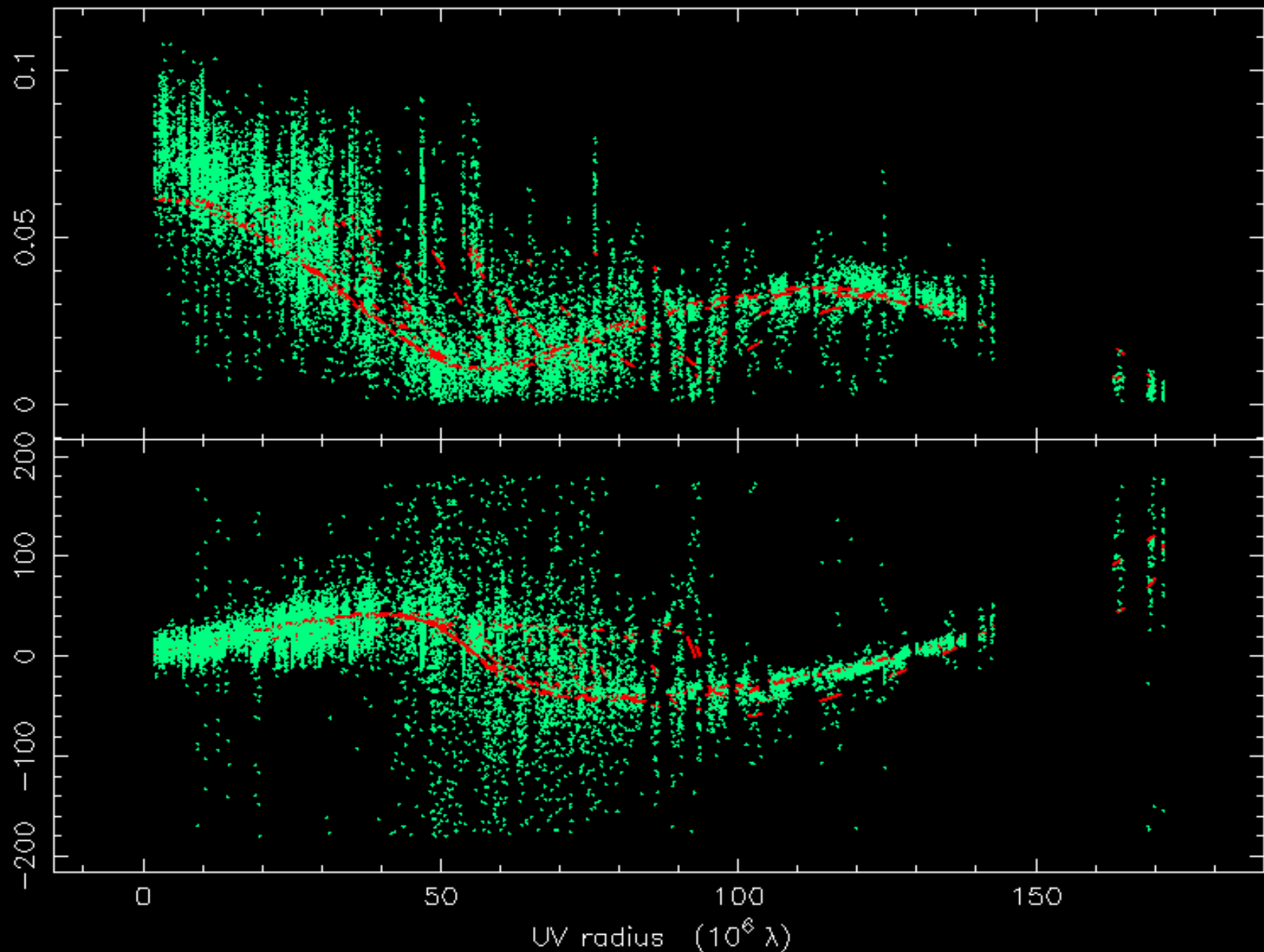
It can be (and must be) checked how the *observed* and the *model* visibility amplitudes and phases are related during the hybrid mapping process, to keep an eye on convergence

- amplitude & phase plots for each VLBI baseline as a function of time (**vplot**)
- correlated flux density & phase vs. projected baseline length plots (**radplot**)

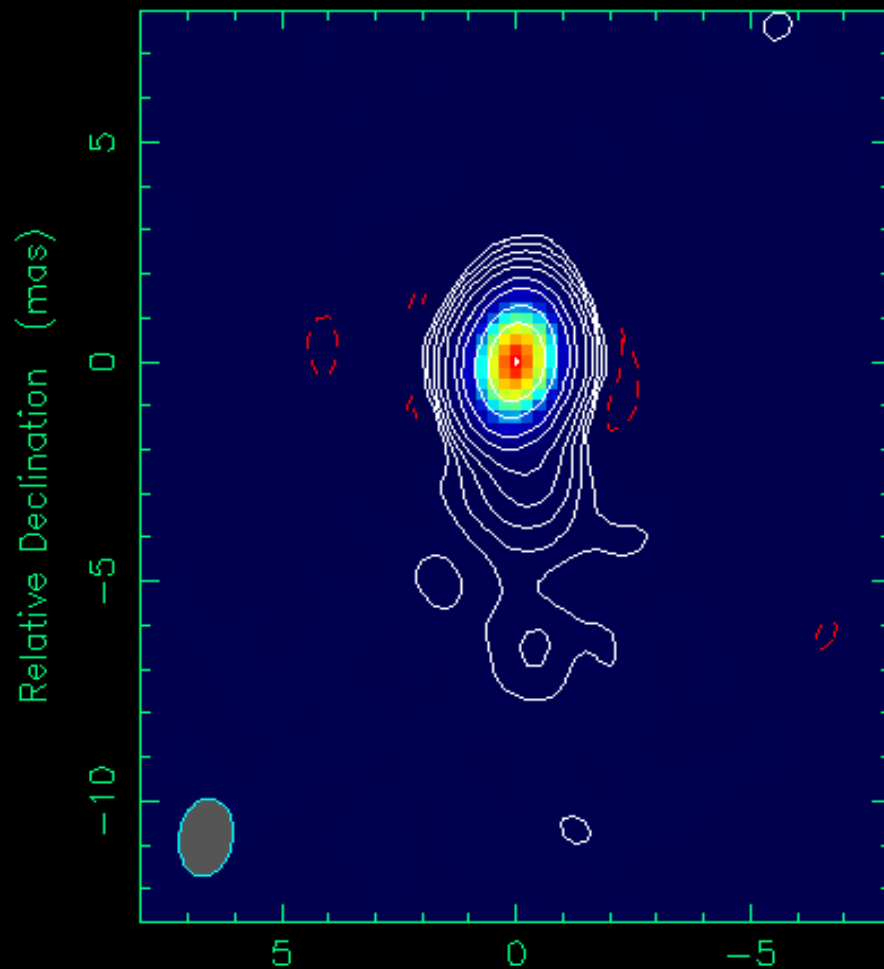
1126+237 1998 Oct 03
Baselines of 1:EB in IF 1, Pol I



1126+237 at 4.976 GHz in I 1998 Oct 03



Clean 1 map. Array: BEFHKLNOP3M
1508+572 at 4.976 GHz 1998 Oct 03



Map center: RA: 15 10 02.922, Dec: +57 02 43.376 (2000.0)

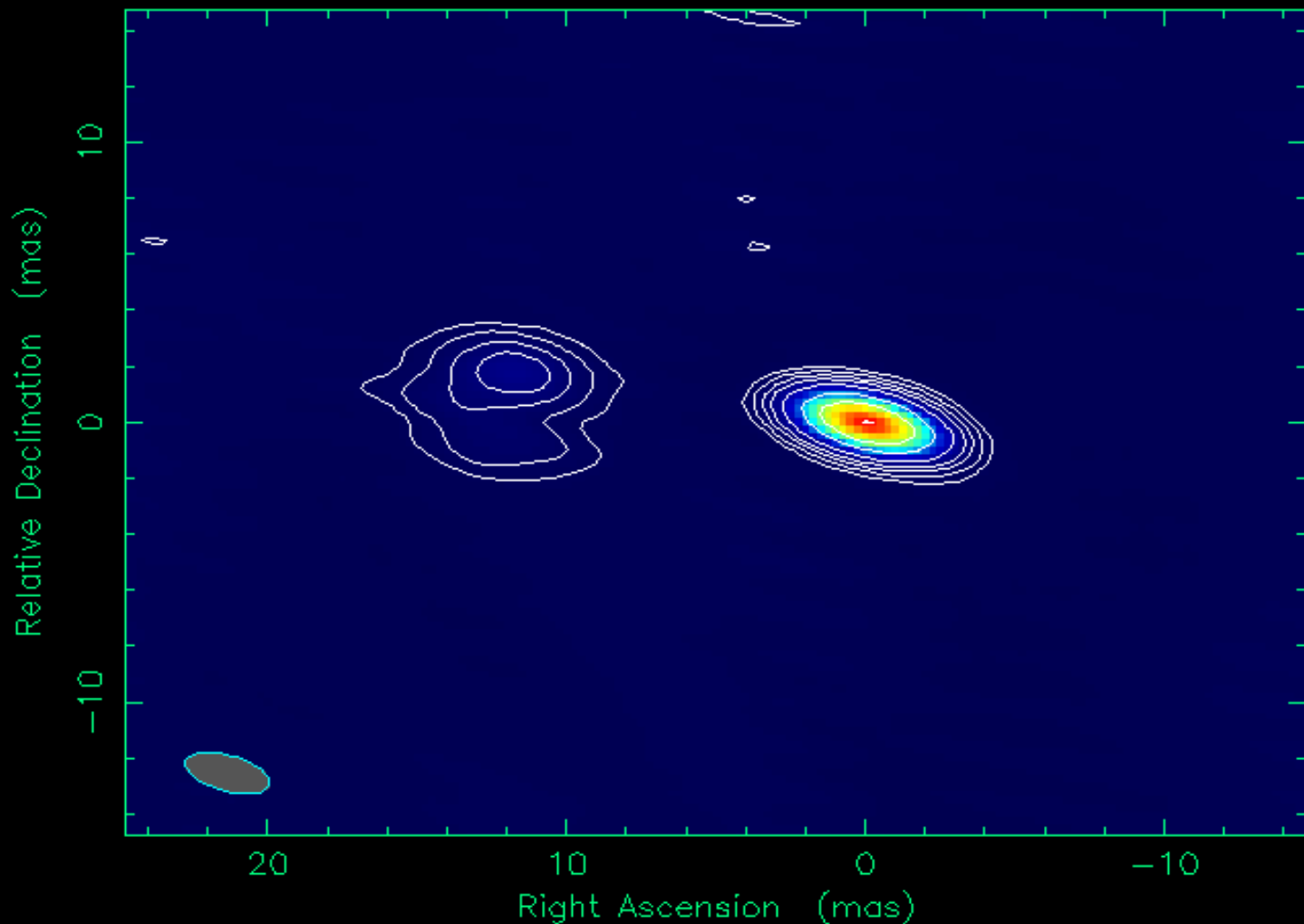
Map peak: 0.363 Jy/beam

Contours %: -0.12 0.12 0.25 0.5 1 2 5 10 25 50 99

Beam FWHM: 1.78 x 1.13 (mas) at -7.74°



Clean Fmap: Array: EVN
J2134-04 at 4.971 GHz 1999 Nov 26

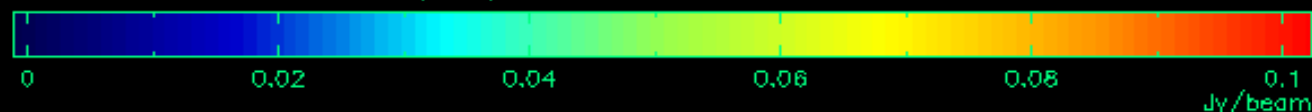


Map center: RA: 21 34 12.020, Dec: -04 19 09.900 (2000.0)

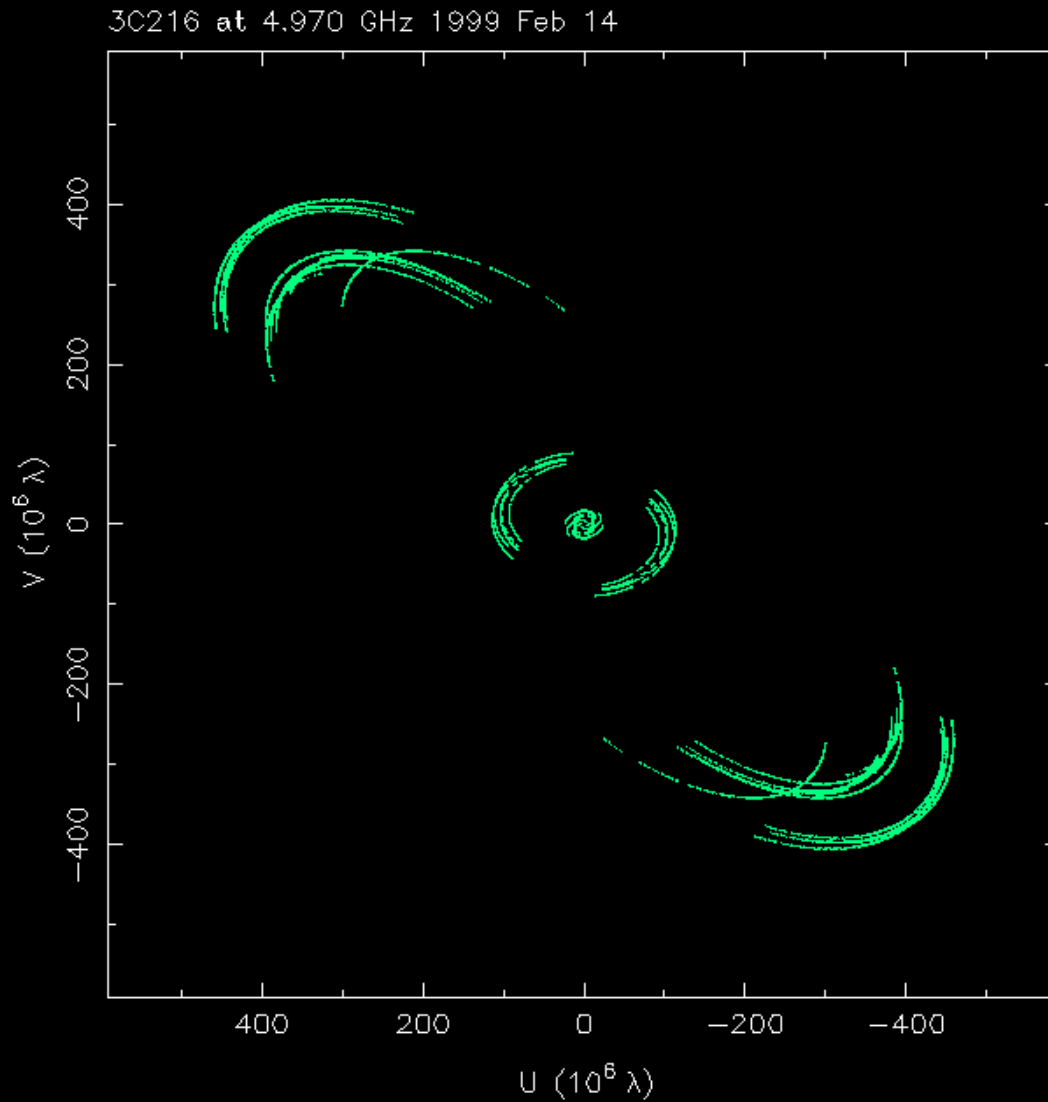
Map peak: 0.102 Jy/beam

Contours %: 0.7 1.5 3 5 10 25 50 99

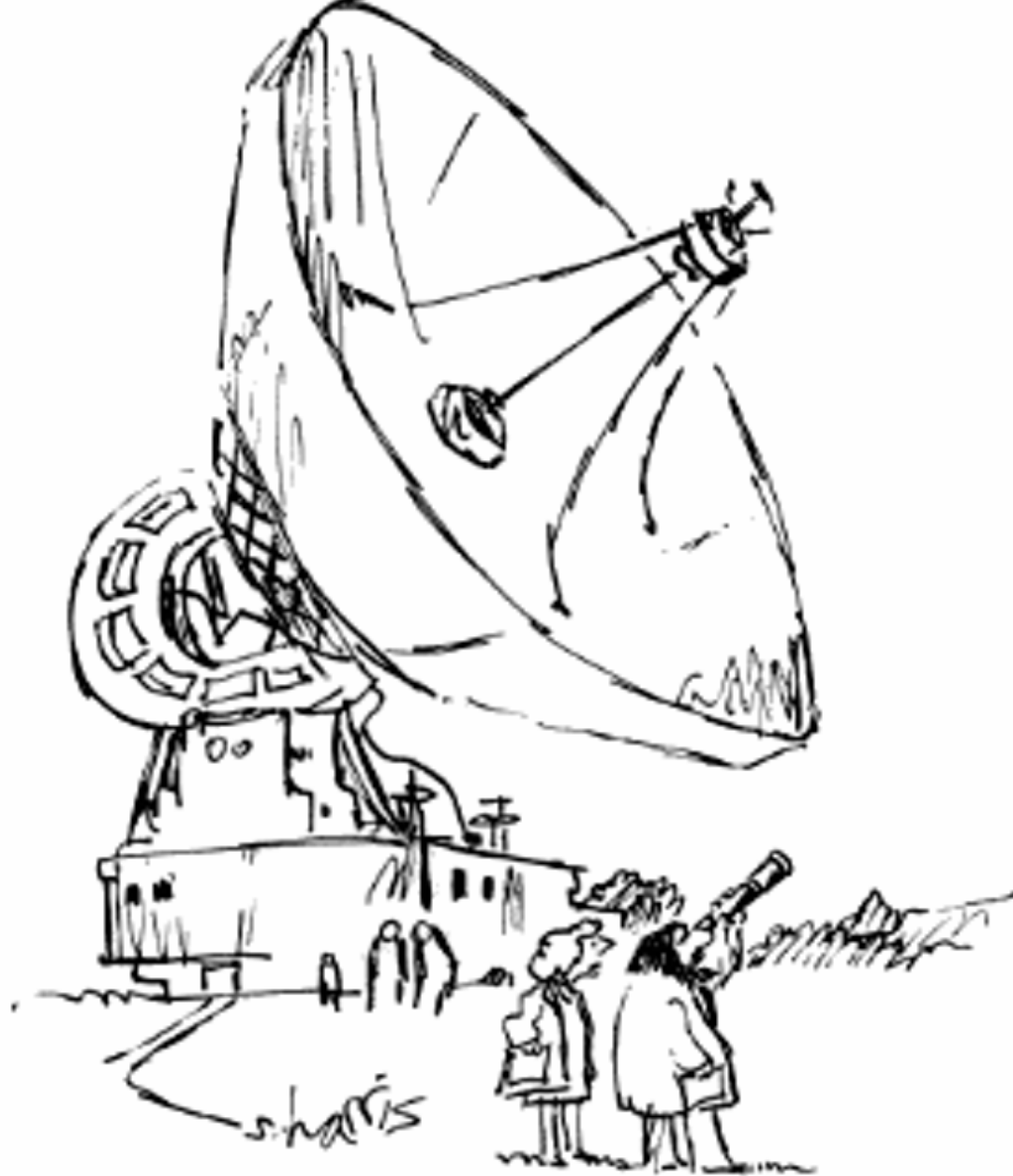
Beam FWHM: 2.95 x 1.26 (mas) at 73.2°



Space VLBI: (u,v) coverages



***Thanks
for your
attention!***



"Just checking."